SETTING THE LIMIT ON AXON GROWTH: MULTIPLE OVERLAPPING MECHANISMS REPRESS THE MAP3K WND/DLK SO THAT GROWTH CONES CAN REMODEL INTO STATIONARY SYNAPTIC BOUTONS

by

ALEXANDER I. FEOKTISTOV

A DISSERTATION

Presented to the Department of Biology
and the Graduate School of the University of Oregon
in partial fulfillment of the requirements
for the degree of
Doctor of Philosophy

March 2016

DISSERTATION APPROVAL PAGE

Student: Alexander I. Feoktistov

Title: Setting the Limit on Axon Growth: Multiple Overlapping Mechanisms Repress the MAP3K Wnd/DLK So That Growth Cones Can Remodel into Stationary Synaptic Boutons

This dissertation has been accepted and approved in partial fulfillment of the requirements for the Doctor of Philosophy degree in the Department of Biology by:

Judith Eisen	Chairperson
Victoria Herman	Advisor
Christopher Doe	Core Member
Phillip Washbourne	Core Member
Bradley Nolen	Institutional Representative

and

Scott L. Pratt	Dean of the Graduate School

Original approval signatures are on file with the University of Oregon Graduate School.

Degree awarded March 2016

DISSERTATION ABSTRACT

Alexander I. Feoktistov

Doctor of Philosophy

Department of Biology

March 2016

Title: Setting the Limit on Axon Growth: Multiple Overlapping Mechanisms Repress the MAP3K Wnd/DLK So That Growth Cones Can Remodel into Stationary Synaptic Boutons

The development of a stereotyped pattern of neural connectivity depends upon the behavior of growth cones, motile structures at the tips of axons that propel axon growth and steer the axon to its targets. When growth cones reach their appropriate target cells, they halt and ultimately remodel into stationary presynaptic boutons. The influence of extracellular cues in directing growth cones to their targets is well studied, but cell-intrinsic factors are also increasingly appreciated for their role in driving much of growth cone behavior.

Dual leucine zipper kinases (DLKs) promote growth cone motility and must be kept in check to ensure normal development. PHR (Pam/Highwire/RPM-1) ubiquitin ligases therefore target DLK for proteosomal degradation unless axon injury occurs. Overall DLK levels decrease during development, but how DLK levels are regulated within a developing growth cone has not been examined. We analyzed the expression of the fly DLK Wallenda (Wnd) in R7 photoreceptor growth cones as they halt at their targets and as they remodel into presynaptic boutons. We found that Wnd protein levels are repressed by the PHR protein Highwire (Hiw) during R7 growth cone halting, as has been observed in other systems. However, during remodeling, Wnd levels are further repressed by a temporally-expressed transcription factor, Tramtrack69 (Ttk69). Previously unobserved negative feedback from JNK also contributes to Wnd repression. We conclude that maturing neurons progressively deploy additional mechanisms to keep DLK off and thereby protect their connectivity. We use live imaging to directly probe the

effects of Wnd and Ttk69 on remodeling R7 growth cones and conclude that Ttk69 coordinates multiple regulators of this process.

Preliminary results indicate that excess Wnd signaling requires the transcription factor Fos to disrupt growth cone remodeling in R7s. This opens up new strategies to identify how Wnd exerts its motility-promoting effects on growth cone cytoskeletons. Additional findings point to a later requirement for Wnd in normal R7 synapse development, suggesting that Wnd expression is not fully silenced in R7s. Further investigation into these findings would greatly advance our understanding of how the neuronal cytoskeleton is regulated as neurons undergo profound morphological and functional changes while developing.

This dissertation includes both unpublished and published co-authored material. This dissertation also includes supplemental movie files, which can be found online and are described in Appendix B.

CURRICULUM VITAE

NAME OF AUTHOR: Alexander I. Feoktistov

GRADUATE AND UNDERGRADUATE SCHOOLS ATTENDED:

University of Oregon, Eugene, OR
Vanderbilt University, Nashville, TN

DEGREES AWARDED:

Doctor of Philosophy, Biology, University of Oregon, 2016
Bachelor of Science, Molecular and Cell Biology, Vanderbilt University, 2007

AREAS OF SPECIAL INTEREST:

Neural Development

Developmental Genetics

PROFESSIONAL EXPERIENCE:

Graduate Teaching Fellow, Department of Biology, University of Oregon, Eugene, OR, 2009-2010, 2013-2016

Research Assistant, Department of Cell and Developmental Biology, Vanderbilt University Medical Center, Nashville, TN, 2007-2009

Undergraduate Researcher, Vanderbilt University Medical Center, Department of Pharmacology, Nashville, TN, 2005-2007

Research Technician, Vanderbilt University Medical Center, Department of Microbiology and Immunology, Nashville, TN, 2003-2005

GRANTS, AWARDS, AND HONORS:

National Institute of Health Genetics Training Grant, University of Oregon 2010-2013

Honors in Molecular Cell Biology, *cum Laude* Vanderbilt University College of Arts and Sciences, 2007

Dean's List, Vanderbilt University College of Arts and Sciences, 2005-2006

National Institute of Health Training Grant, Vanderbilt University Medical Center, Department of Microbiology and Immunology Summer Undergraduate Research Program, 2004.

PUBLICATIONS:

Feoktistov, A. I. and Herman, T. G. (manuscript provisionally accepted February, 2016) Wallenda/DLK protein levels are temporally regulated by Tramtrack69 to allow remodeling of growth cones into boutons. *Development.*

Efimova, N., Grimalidi, A., Bachmann, A., Frye, K. Zhu, X**., Feoktistov, A.**, Straube, A., and Kaverina, I. (2014). Podosome-regulating kinesin KIF1C translocates to the cell periphery in a CLASP-dependent manner. *Journal of Cell Science*. Dec 15; 127(24): 5179-88.

Chung, C.Y., **Feoktistov, A.**, Hollingsworth R.J., Rivero, F., and Mandel, N.S. (2013). An attenuating role of a WASP-related protein, WASP-B, in the regulation of F-actin polymerization and pseudopod formation via the regulation RacC during Dictyostelium chemotaxis. *Biochemical and Biophysical Research Communication*. Jul 12;436(4):719-24.

LaFever, L., **Feoktistov, A.**, Hsu, H.J., and Drummond-Barbosa, D. (2010). Specific roles of Target of Rapamycin in the control of stem cells and their progeny in the Drosophila ovary. *Development.* Jul; 137(13):2117-26.

ACKNOWLEDGMENTS

I am profoundly grateful to my advisor, Tory, for her mentorship, guidance and most of all her investment in my success. Additional thanks are due to members of the Herman Lab, whose varied skills, interests, and ideas made hours spent dissecting fruit fly brains that much more enjoyable. Feedback on homebrew was also greatly appreciated. I want to specifically thank Jon Kniss for stewarding the early days of my project following up on his work. Special thanks also go to an undergraduate honors thesis student I mentored, Alex Whitebirch, for his tireless efforts to identify targets of Ttk69. I am proud to have been there at the beginning of what is likely to be a productive career. I also want to thank Eric Lyons for his irreplaceable role in managing much of the day-to-day running of the Herman Lab and I am especially grateful for his help in assembling the computer which was used to generate an overwhelming majority of the work presented below. Finally I am grateful for the love and support of friends and brew-crew members near and far, and am especially grateful to my family for always motivating me to succeed.

I dedicate this work to my parents who have always been an inspiration to me.

TABLE OF CONTENTS

LIST OF FIGURES

CHAPTER I

INTRODUCTION TO THE ROLE OF GROWTH CONE MOTILITY IN THE ESTABLISHMENT OF NEURONAL CIRCUITRY

Preface

The human brain is by far the most complex and poorly understood organ. Neurons are the basic informational unit of the brain, and these cells detect, transmit, and encode stimuli from the world around us. They form networks that endow us with the cognitive abilities that allow us to do everything from learning to avoid noxious stimuli to forming social bonds that sustain civilization. Information in the brain is encoded through electrical impulses propagated by the opening of ion channels, and transmitted from neuron to neuron by specialized connections called synapses. Most synapses are chemical synapses; an electrical stimulus from the presynaptic cell is translated into a chemical message by voltage-mediated exocytosis of neurotransmitter-containing vesicles at the presynaptic site. Binding of neurotransmitter to specific receptors on the postsynaptic site relays the message to the postsynaptic cell. Some neurotransmitter receptors are ion channels which open upon ligand binding causing a change in membrane potential in postsynaptic cells, thus propagating the electrical message. Other neurotransmitter receptors trigger a signal transduction cascade which often leads to changes in excitability of the postsynaptic site. Human brains contain billions of neurons and trillions of synapses arranged in a complex, but stereotyped circuitry. How is this complexity assembled and organized?

Overview of how neural circuits develop

Much of our understanding of how this stereotyped circuitry is built comes from studying the genes required for forming this circuitry. The cells that will give rise to the nervous system are specified by exposure to specific morphogens during gastrulation. Neuronal stem cells within this population undergo self-renewing asymmetric divisions, and after amplifying divisions by progenitor cells, neurons differentiate and undergo profound morphological changes. They become polarized and specialized processes

called neurites extend from the cell body. One neurite differentiates into the axon, and typically contains most of the presynaptic sites. Other neurites will differentiate into dendrite and will typically contain most of the postsynaptic sites.

Shortly after neurites differentiate, microtubules in the axon shaft become polarized, with their plus ends oriented away from the cell body (Stiess and Bradke, 2011). At the tip of the axon is a specialized subcellular structure called the growth cone. The growth cone propels the growing axon and steers it to its proper targets –a necessary function for assembling the correct circuitry (Lowery and Van Vactor, 2009). As growth cones navigate their way to their targets, they exhibit a dynamic range of morphologies that are strongly correlated with their behavior; growth cones are often streamlined when advancing, paused growth cones are expanded, retracting growth cones appear collapsed, and turning growth cones engorge in new directions (Godemont et al., 1994). These behaviors are driven by the dynamic rearrangement of the growth cone cytoskeleton. Actin filaments project from the growth cone in fine processes called filopodia which probe the extracellular space. In between the filopodia is a mesh-like network of branched actin that forms the lamellipodium-like veil. At the central core of the growth cone is a bundle of microtubules, most of which are constrained by an actin-myosin ring, though some microtubules escape this contractile ring and extend into filopodia; these are called pioneer microtubules (Lowery and Van Vactor 2009; Vitriol and Zheng, 2012). The ability of microtubules to explore the growth cone is what drives the rapid growth of axons when compared to dendrites, and the orientation of pioneer microtubules is strongly associated with the direction of axon extension (Stiess and Bradke, 2011; Bearce et al., 2015).

Extracellular molecules act as guidance cues by binding to specialized receptors triggering polymerization of the growth cone cytoskeleton in response to attractive cues or instead depolymerization in the case of repulsive cues (Lowery and Van Vactor, 209; Vitriol and Zhang, 2012). These guidance molecules can be diffusible molecules secreted from neuronal targets, transmembrane proteins expressed by "guidepost" cells, or secreted molecules imbedded in the extracellular matrix along which the neuron migrates. This is how the growth cone steers the extending axon. Active propulsion is achieved by a three step process: 1) polymerizing actin propels the leading edge of the growth cone

forward. 2) The microtubule core of the axon shaft engorges into the extended leading edge, which is caused by a breakdown of the actin-myosin contractile ring. 3) Growth is consolidated by the reformation of the actin-myosin ring, which re-establishes the central bundle of microtubules that makes up the axon shaft. This cycle repeats to drive persistent growth.

How is growth cone motility reduced so that neurons can establish initial connectivity?

When axons arrive at their terminal targets, growth cones collapse, lose motility, and remodel into ellipsoid synaptic boutons that lack filopodia and other features characteristic of growth cones. Failure to properly limit growth cone motility leads to excessive axon extension that disrupts the normal circuitry. Though the mechanisms that guide growth cones to their targets are well studied, how growth cones transition from a motile state into stable synaptic boutons is unclear. Trans-synaptic signaling is known to promote assembly of synaptic components, but some neurons form synapses *en passant* suggesting that separate mechanisms must exist to signal a decrease in growth cone motility during a particular developmental window. A potential mechanism for how neurons might achieve this is by a temporal decrease in the abundance or activity of cell-intrinsic factors promoting growth cone motility. Alternatively temporal activation of cell-intrinsic factors that restrict growth cone motility would achieve the same result. Insight into this problem comes from recent studies of axon regeneration, as the ability of neurons to regenerate depends on their ability to reform motile growth cones. It has long been thought that expression of inhibitory extracellular molecules within the central nervous system (CNS), but not the peripheral nervous system (PNS) prevents CNS axons from regenerating yet PNS axons are capable of doing so (Case and Tessier-Levine, 2005). However, it is now known that differences in expression of cell-intrinsic factors can account for different abilities to regenerate (Goldberg, 2004; Moore et al., 2011; Mar et al., 2014; Steketee et al., 2014). For example, neurons within the dorsal root ganglion (DRG) extend two branches: one branch that extends to the periphery and is part of the PNS and another that extends through the spinal cord and is part of the CNS. Studies show that a conditioning lesion on the PNS axon branch triggers changes in cell-intrinsic

gene expression that allows the CNS branch to regenerate a motile growth cone, an ability these axons lack in the absence of a conditioning lesion (Hoffman, 2009). Furthermore, it is known that neurons lose the ability to regenerate motile growth cones as they age, in particular after the end of embryonic development (Goldberg et al., 2004; Byrne et al., 2014). Cell-intrinsic changes in gene expression in aging neurons can account for some of this decline (Byrne et al., 2014).

However it is not clear whether cell-intrinsic changes in gene expression occur when the neuronal circuitry is first being established or after initial connectivity is already assembled. I asked whether there might be a factor that promotes growth cone motility whose expression is specifically limited when growth cones decrease motility and transition to ellipsoid synaptic boutons. An appealing candidate was the Dual Leucine-zipper Kinase (DLK) for its known role in promoting growth cone motility in developing neurons and its necessity and sufficiency for regenerating motile growth cones (Nakata et al., 2005; Collins et al 2006; Hirai et al., 2006; Lewcock et al., 2007; Eto et al., 2010; Xiong et al., 2010; Nix et al., 2011; Wang and Jin; 2011; Klinedinst et al., 2013). In the next chapter, I describe my co-authored study, which was provisionally accepted to the journal *Development*, asking whether DLK is limited to promote a decrease in growth cone motility of neurons in the process of establishing their connectivity and if so, by what mechanism. In subsequent chapters, I describe unpublished co-authored work asking how Wnd and Ttk69 exert their effects on the growth cone cytoskeleton.

CHAPTER II

WALLENDA/DLK PROTEIN LEVELS ARE TEMPORALLY REGULATED BY TRAMTRACK69 TO ALLOW REMODELING OF R7 GROWTH CONES INTO BOUTONS

The work described in this chapter was provisionally accepted for publication in the journal *Development* in February, 2016. Alexander I. Feoktistov and Tory G. Herman designed and interpreted the experiments, designed the figures and wrote the manuscript. Alexander I. Feoktistov performed all of the experiments.

Introduction

The pattern of connectivity among neurons depends upon the behavior of growth cones, motile structures at the tips of axons. Growth cones extend, turn, pause, and retract as they navigate specific pathways, halt upon contacting the appropriate target cells, and ultimately remodel into stationary presynaptic boutons. While much of this behavior is regulated by extrinsic cues (Lowery and Van Vactor, 2009; Vitriol and Zheng, 2012), cell-intrinsic factors also play a critical role in regulating the dynamic rearrangement of the growth cone cytoskeleton (Goldberg, 2004; Moore et al., 2011; Mar et al., 2014; Steketee et al., 2014). In particular, the conserved mitogen-activated protein kinase kinase kinase (MAP3K) DLK is a potent cell-intrinsic regulator of microtubule dynamics. DLK levels increase in response to axon injury and promote growth cone assembly and extension by activating the MAPKs JNK and p38 (Nakata et al., 2005; Collins et al 2006; Hirai et al., 2006; Lewcock et al., 2007; Eto et al., 2010; Xiong et al., 2010; Nix et al., 2011; Klinedinst et al., 2013). While loss of *dlk* has only subtle effects on normal development (Collins et al., 2006; Fernandes et al., 2011; Shin and DiAntonio, 2011; Wang et al., 2013), DLK overexpression cell-autonomously disrupts axon connectivity by causing growth cones to extend beyond their targets (Lewcock, et al., 2007; Wang et al., 2013; Baker et al., 2014; Opperman and Grill, 2014). DLK activity is therefore

normally limited by PHR family E3 ubiquitin ligases, which target DLK for proteosomal degradation in the absence of injury (Liao et al., 2004; Nakata et al., 2005; Collins et al., 2006; Wu et al., 2007; Brace et al., 2014). DLK levels have been reported to decrease during development (Collins et al., 2006; Eto et al., 2010), suggesting that PHR or other mechanisms progressively downregulate DLK as neurons form stable connections. However, how DLK levels are regulated during the course of an individual growth cone's development has not been examined in detail.

To test whether DLK is differentially regulated over the course of normal growth cone development, we used the R7 photoreceptor neurons in the *Drosophila* eye. R7 growth cone motility decreases in two main phases (Ting et al., 2005; Kniss et al., 2013; Chen et al., 2014; Özel et al., 2015): (1) after arriving in the optic lobe, R7 growth cones halt within a specific target layer; they no longer actively move forward but do remain expanded and continue to extend and retract multiple small processes; (2) as the R7 axons continue to lengthen by passive stretch growth, the R7 growth cones gradually decrease in volume, their processes decrease in number and motility, and they ultimately become smooth boutons that lack processes. We set out to determine how DLK/Wnd levels are regulated during R7 growth cone development. We expected that Wnd would be repressed by PHR/Hiw during phase (1) halting, as has been observed in other systems. And we hypothesized that Wnd might then be further downregulated to allow phase (2) remodeling to occur.

Here we show that Wnd levels in R7 growth cones are downregulated by a novel, Hiw-independent mechanism during phase (2) remodeling. As in other systems, R7 growth cones do require Hiw during phase (1) to repress and thereby prevent Wnd from disrupting R7 growth cone halting. However, loss of *hiw* alone has no effect on phase (2) remodeling. Instead, Wnd levels are additionally repressed by Ttk69, a transcriptional repressor that we previously showed is specifically expressed and required in R7s during growth cone remodeling (Kniss et al., 2013). In contrast to the JNK-dependent positive feedback that has been observed during axon injury in mammalian cell culture (Huntwork-Rodrigues et al., 2013), we found that during both phases of R7 development, Wnd protein levels are additionally repressed by JNK-dependent negative feedback. We

use live imaging to show that Wnd overexpression and Ttk69 loss have overlapping but distinct effects on R7 growth cone remodeling. We conclude that neurons may use temporal factors to progressively limit DLK expression as their connections become more stable. And we conclude that in R7s the temporal factor Ttk69 promotes growth cone remodeling by repressing multiple cell-intrinsic regulators of growth cone dynamics.

Results

Wnd protein is downregulated independently of Hiw in R7 growth cones that are remodeling into presynaptic boutons

Previous work has shown that average levels of DLK decrease during development. One possibility is that individual neurons progressively downregulate DLK as their growth cones lose motility. To test this, we examined the levels of DLK/Wnd protein in R7 growth cones. We anticipated that, as in other systems, R7 growth cones would use Hiw to repress Wnd as they halt at their target layer (24 h APF). However, we wanted to know whether Wnd is repressed further in R7 growth cones as they remodel into stationary boutons (60 h APF). We therefore used anti-Wnd antibodies to quantify Wnd protein levels in R7 growth cones at these two timepoints; we were unable to quantify anti-Wnd staining in actively extending R7 growth cones because of their location and orientation. At 24 h APF, we found that anti-Wnd staining in R7 growth cones is indistinguishable from that in *wnd* deletion mutants (Fig. 1A,A',E) but that loss of *hiw* increases Wnd levels significantly (Fig. 1B,B',E). We conclude that, as expected, Hiw is required to repress Wnd during R7 growth cone halting. We note that loss of *hiw* also increases anti-Wnd staining in R8 growth cones at this time (Fig. 1A-B', data not shown).

We next examined R7 growth cones at the 60 h APF timepoint. Again, anti-Wnd staining in wild type is low and indistinguishable from that in *wnd* deletion mutants (Fig. 1C,C',E), indicating that any decrease in Wnd in wild-type R7 growth cones is below our level of detection with these antibodies. However, we found that loss of *hiw* causes a much smaller increase in Wnd levels at 60 h APF (Fig. 1D,D'.E) and that Wnd levels

therefore decrease significantly in *hiw* mutant R7 growth cones between 24 and 60 h APF. We conclude that Wnd is downregulated by a Hiw-independent mechanism as R7 growth cones remodel into stationary boutons.

During R7 growth cone halting, Wnd must be repressed by Hiw to prevent extension beyond the correct target layer

Having found that R7 growth cones use an additional mechanism to repress Wnd during R7 growth cone remodeling, we wanted to compare the effects of increased Wnd on remodeling and halting. We first examined R7 growth cone halting (24 h APF). We anticipated that, as in other systems, an increase in Wnd might cause R7 growth cones to project beyond their normal target layer (Schaefer et al., 2000; Lewcock et al., 2007; Yan et al., 2009; Wang et al., 2013; Baker et al., 2014; Opperman and Grill, 2014). We used either the photoreceptor-specific *chaoptin-Gal4* (*chp-Gal4*) driving *UAS-mCD8-GFP* to label R7 and R8 axons (Fig. 2A-D') or the R7-specific *PM181-Gal4* driving *UAS-mCD8-GFP* to label R7 axons only (Fig. S2A-B'; see Appendix A for all Supplementary Figures and Legends). We found using either marker that R7 growth cones in *hiw* mutants do halt at the correct target layer but are elongated [a hallmark of forward-moving growth cones (Godemont, 1994)] and frequently extend long, thin processes beyond their targets (Fig.

Figure 1 (next page). Wnd protein is downregulated independently of Hiw in R7 growth cones as they remodel into presynaptic boutons.
Pupal medullas (29°C) in which R7 and R8 axons are labeled with anti-Chp (A-D) and anti-Wnd (A'-D').
Scale bars are 5 μm. (E) Quantification of anti-Wnd levels in R7 growth cones. n=brains, error bars represent SEM, and **p<0.001, ***p<0.0001 based on two-tailed t-tests. n.d.= no data. n=14, 16, 5, 6, 10, 17, and 8, respectively. At 24 h APF (A,A'), wild-type R7 growth cones have halted at their medullar target layer but remain expanded. (B,B') *hiw* mutant R7 growth cones contain significantly more anti-Wnd staining (E) and extend processes beyond their target layer (arrow heads). However, by 60 h APF, *hiw* mutant R7 growth cones are indistinguishable from wild type and contain significantly less anti-Wnd staining than at 24 h APF (C-E). The level of anti-Wnd staining in wild-type R7 growth cones is indistinguishable from that in *wnd* deletion mutants at each timepoint, indicating that R7 growth cones normally express little or no Wnd protein during both halting and remodeling. Using *chp-Gal4* to drive expression of dominant-negative JNK (JNK^{DN}) in R7s also significantly increases anti-Wnd staining in their growth cones at 24 h APF, indicating that JNK provides negative feedback to Wnd (see Fig. 2).

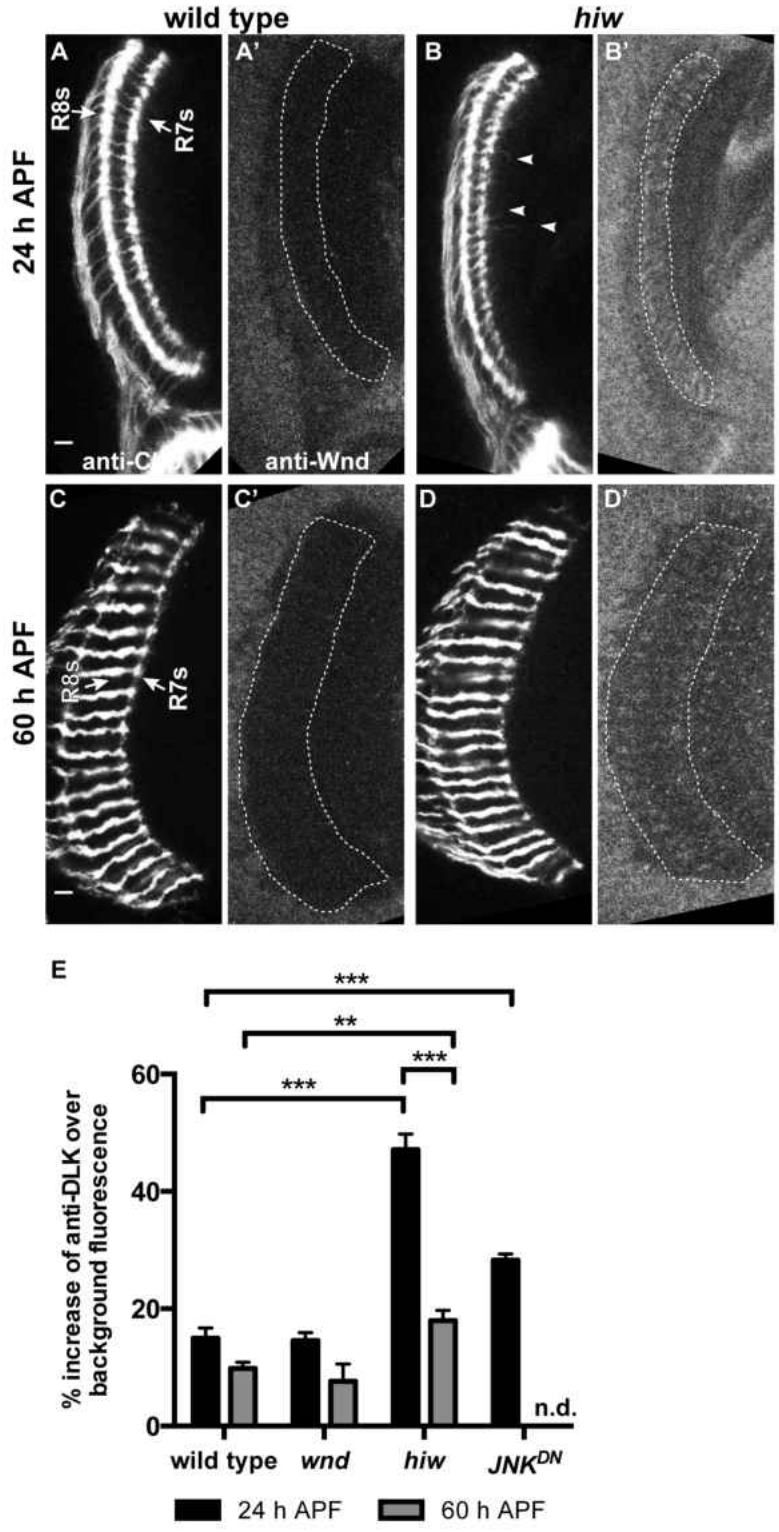
wild type
hiw
A
A'
B
B'
C
C'
D
D'
24 h APF
60 h APF
R8s
R7s
anti-Wnd
E
% increase of anti-DLK over background fluorescence
60
40
20
0
***
**
***
***
n.d.
wild type
wnd
hiw
JNK^DN
24 h APF
60 h APF

2B,B',E,F). Because PHR proteins can have DLK-independent effects (Burgess et al., 2004; D'Souza et al., 2004; McCabe et al., 2004; Collins et al., 2006; Bloom et al., 2007; Grill et al., 2007; Li et al., 2008; Brace et al., 2014), we verified that the upregulation of Wnd in *hiw* mutants is responsible for disrupting R7 growth cone halting: loss of *wnd* from *hiw* mutants fully rescues the overextensions (Fig. 2C-F), and driving increased expression of Wnd in wild-type R7s is sufficient to cause them (Fig. 2G, Fig. S2E,E'). We conclude that Hiw is required to repress Wnd in R7 growth cones to promote normal halting. As in other systems (Collins et al., 2006; Fernandes et al., 2011; Shin and DiAntonio, 2011; Wang et al., 2013), loss of *wnd* does not disrupt R7 growth cone morphology or connectivity (Fig. 2C,C',E,F; data not shown).

During R7 growth cone halting, Wnd is also repressed by negative feedback from JNK

While examining the role of increased Wnd levels in R7 growth cone halting, we identified a second, unexpected mechanism by which Wnd is repressed at this timepoint. To test whether Wnd disrupts R7 halting by acting upstream of JNK (Hirai et al., 2002;

Figure 2 (next page). R7 growth cones require Hiw to repress Wnd as they halt at their target layer.
(A-D') 24 h APF pupal medullas (25°C) in which R7 and R8 axons are labeled with *chp-Gal4, UAS-mCD8-GFP* (green) and anti-Chp (red). Scale bars are 5 μm. A'-D' are enlargements of the boxed regions in (A-D) with enhanced brightness. Arrows indicate the R7 and R8 target layers. (E-G) Quantifications of R7 growth cone phenotypes. n=brains, error bars represent SEM. (E,F) n=9, 8, 11, and 11, respectively. (G) n=7, 8, 7, and 12, respectively. *hiw* mutant R7 growth cones are elongated (B,B',E; two-tailed t-test) and extend processes beyond their target layer (arrowheads; processes of at least 3 μm are quantified in F; two-tailed t-test). R8 growth cones occasionally terminate between the R8 and R7 target layers (arrow; 1.7±0.6% versus <0.08% in wild type; See Fig. S1B,B'). Loss of *wnd* has no effect on wild-type R7 growth cones (C,C',E,F) but restores the morphology of *hiw* mutant R7 growth cones to that of wild type (D-F; one-tailed but restores the morphology of *hiw* mutant R7 growth cones to that of wild type (D-F; one-tailed t-tests, *p<0.01). R8 growth cones occasionally extend beyond their target layer in both *wnd* (data not shown) and *hiw; wnd* mutants (arrow). (G) Using *chp-Gal4* to drive co-expression of Wnd (wnd^{OE}) and RFP (as a control for *UAS* copy number) is sufficient to disrupt R7 growth cone halting. Co-expressing Wnd with JNK^{DN} ameliorates this defect (G, ***p<0.0001, Fig. S2). (H) Model summarizing the roles of Hiw, Wnd, and JNK as R7 growth cones halt at their target layer.

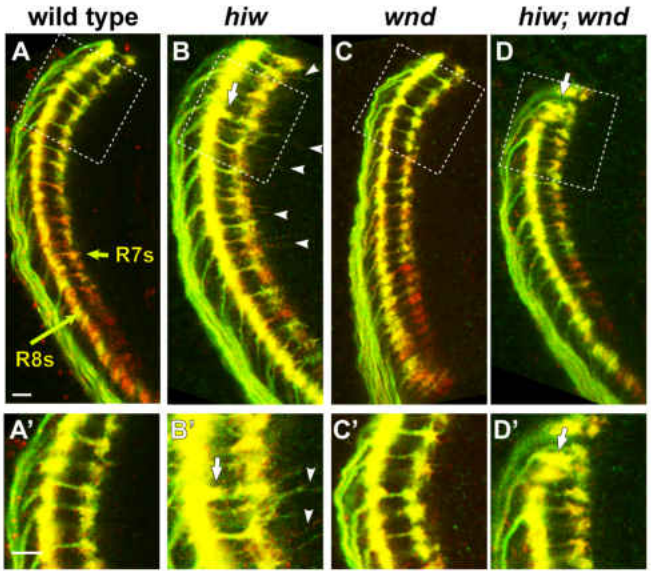
wild type
hiw
wnd
hiw; wnd
A
B
C
D
R7s
R8s
A'
B'
C'
D'

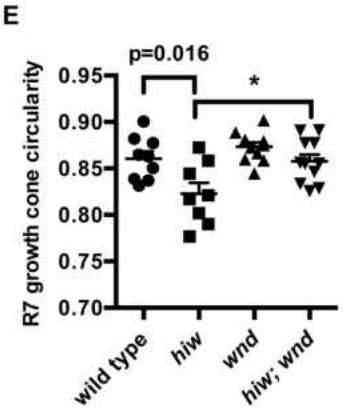
E
p=0.016
*
R7 growth cone circularity
0.95
0.90
0.85
0.80
0.75
0.70
wild type
hiw
wnd
hiw; wnd

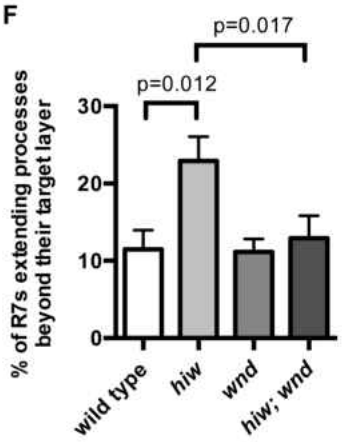
F
p=0.017
p=0.012
% of R7s extending processes beyond their target layer
30
20
10
0
wild type
hiw
wnd
hiw; wnd

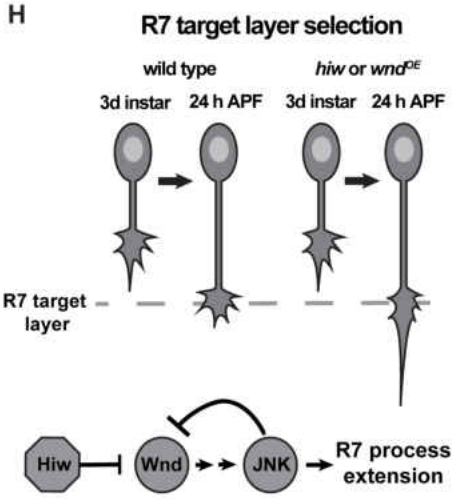
H
R7 target layer selection
wild type
hiw or wnd^OE
3d instar
24 h APF
3d instar
24 h APF
R7 target layer
Hiw
Wnd
JNK
R7 process extension

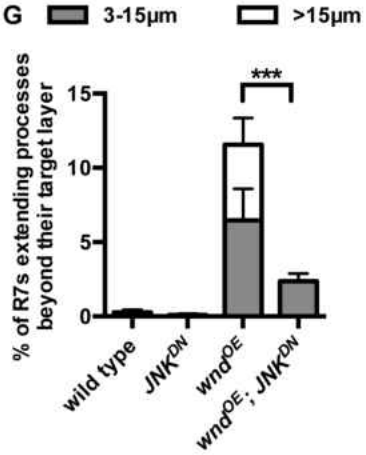
G
3-15µm
>15µm
***
% of R7s extending processes beyond their target layer
15
10
5
0
wild type
JNK^DN
wnd^OE
wnd^OE; JNK^DN

Collins et al., 2006; Eto et al., 2010; Yan and Jin, 2012), we co-expressed Wnd with a dominant-negative version of JNK (JNK^{DN}; Weber et al., 2000). We found, indeed, that JNK^{DN} almost completely eliminates the processes that Wnd-overexpressing R7 growth cones extend beyond their target layer (Fig. 2G, Fig. S2F,F'), indicating that Wnd acts upstream of JNK in this process. To our surprise, we noticed that expressing JNK^{DN} in R7s also significantly increases Wnd levels in R7 growth cones, although to a lesser extent than loss of *hiw* (Fig. 1E). Consistent with our finding that Wnd requires JNK to disrupt R7 growth cone halting, JNK^{DN} does not disrupt R7 growth cone halting, despite the increase in Wnd (Fig. S2D,D'). We conclude that during R7 growth cone halting, JNK acts in a negative feedback loop that contributes to restricting Wnd levels (Fig. 2H). Mammalian JNK has recently been shown to act in a positive feedback loop to increase DLK levels during axon regeneration (Huntwork-Rodriguez et al., 2013). However, JNK-mediated negative feedback has not previously been reported.

As R7 growth cones remodel into boutons, Wnd must be repressed to prevent a different defect: extension within the correct target layer

We next wanted to determine the effects of increased Wnd on R7 growth cones that are remodeling into boutons. We again used the *chp* promoter driving GFP expression to label R7 and R8 axons but examined two later timepoints that span the remodeling process: (1) 40 h APF, when wild-type R7 axon terminals first start assembling active zones but are still expanded and extend multiple thin processes; and (2) 60 h APF, by which time R7 terminals have many active zones, are condensed, and extend fewer processes (Ting et al., 2005; Chen et al., 2014; Özel et al., 2015; see below). We first examined *hiw* mutants, since we found that Hiw loss modestly increases Wnd levels at 60 h APF (Fig. 1). We hypothesized that the defect in R7 growth cone halting in *hiw* mutants might worsen over time. However, we found instead that R7 axon terminals in *hiw* mutants are indistinguishable from wild-type at both 40 and 60 h APF (Fig. 3A,B,D,E,G,H). In particular, they no longer extend processes beyond their target layer (Fig. 3G). We conclude that, despite the increased Wnd levels that are still present in *hiw* mutant R7 growth cones, the earlier effects on R7 growth cone morphology are somehow later corrected and remodeling proceeds normally. One possiblity is that older R7 growth

cones simply become insensitive to increased Wnd levels. Alternatively, perhaps the Hiw-independent decrease in Wnd levels that we observed between halting (24 h APF) and remodeling (60 h APF) provides protection to remodeling R7 growth cones.

To distinguish between these possibilities, we again used *chp-Gal4* to drive increased expression of Wnd in wild-type R7 neurons - the same manipulation that disrupts R7 growth cone halting at 24 h APF (Fig. 2G, Fig. S2E,E'). We found that

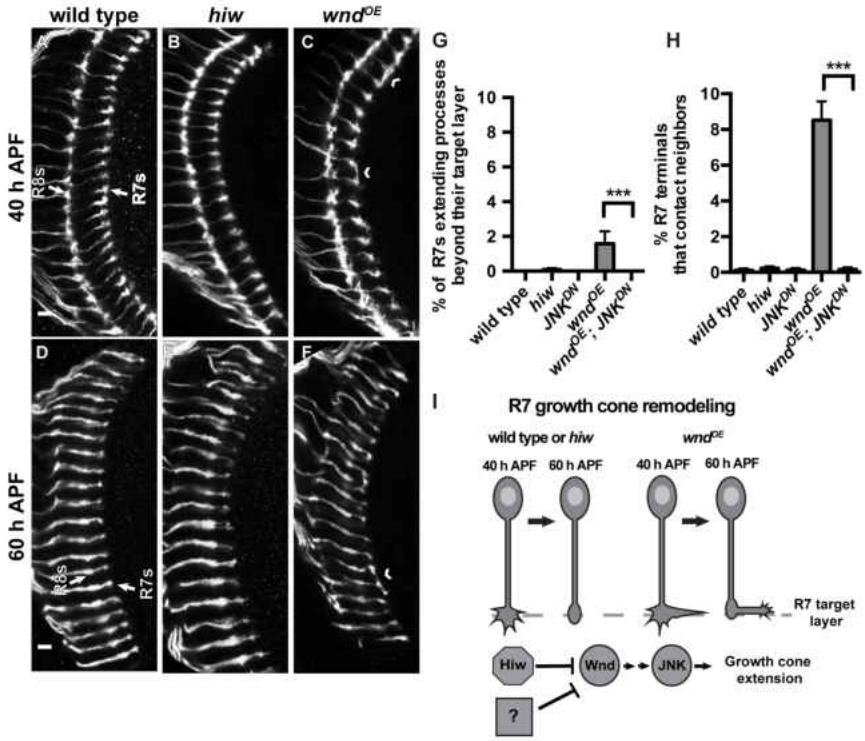

Figure 3. R7 growth cones do not require Hiw as they remodel into presynaptic boutons, yet Wnd overexpression disrupts this process.
(A-F) Pupal medullas (25°) in which R7 and R8 axons are labeled with *chp-Gal4, UAS-EB1-GFP* (white). Scale bars are 5 µm. Arrows indicate the R7 and R8 target layers. (G,H) Quantification of R7 growth cone phenotypes at 48 h APF (29°C). n=brains, error bars represent SEM. n=8, 7, 11, 7, and 10, respectively. By 40 h APF (A,B), wild-type and *hiw* mutant R7 axon terminals are indistinguishable. The same is true at 60 h APF (D,E). By contrast, using *chp-Gal4* to drive co-expression of Wnd and control RFP causes R7 axon terminals to contact adjacent R7 terminals (chevrons; H) and, occasionally, extend processes beyond their target layer (G). These defects are eliminated by co-expressing Wnd with JNK^{DN} (G,H; ***$p<0.0001$). (I) Model summarizing the roles of Hiw, Wnd, and JNK as R7 growth cones remodel into boutons.

despite the prolonged high Wnd levels, the R7 growth cone halting defect is substantially corrected by 48 h APF: significantly ($p<0.001$) fewer R7 axon terminals extend processes beyond their target layer at the later timepoint (Fig. 3C,G). However, a significant number of R7 axon terminals instead extend laterally and contact adjacent neighbors (Fig. 3C,H). Co-expressing JNK^{DN} together with Wnd completely ameliorates both defects (Fig. 3G,H). We conclude that older R7s are sensitive to increased Wnd, suggesting that the Hiw-independent mechanism that contributes to repressing Wnd during remodeling serves a protective purpose (Fig. 3I). While the remodeling defect caused by increased Wnd is different from the earlier halting defect, Wnd acts through JNK in each case.

Wnd overexpression and Ttk69 loss cause similar defects in R7 growth cone remodeling

We previously found that a transcriptional repressor, Ttk69, is specifically expressed and required in remodeling R7 growth cones to prevent a remodeling defect similar to that caused by Wnd overexpression (Kniss et al., 2013). To directly compare the effects of Wnd and Ttk69 on individual R7 growth cones, we used the *GMR-FLP*/MARCM technique to generate GFP-labeled wild-type R7s (Fig. 4A,E,H), GFP-labeled wild-type R7s that overexpress Wnd (Fig. 4B,C,F,I), and GFP-labeled *ttk69* mutant R7s (Fig. 4D,G,J). Consistent with our previous results, we found that at 24 h APF, R7s overexpressing Wnd have elongated growth cones that extend processes beyond their target layer (Fig. 4B); however, some are instead expanded laterally (Fig. 4C), a defect that was obscured when all R7 growth cones were labeled. At this early timepoint, Ttk69 is not yet expressed in R7s and *ttk69* mutant R7 growth cones are normal (Kniss et al., 2013; Fig. 4D). By 48 and 60 h APF, R7s overexpressing Wnd frequently extend some distance laterally, causing overlap with multiple neighboring wild-type R7 terminals (Fig. 4F,I); some also extend branches within the M1 layer (data not shown). These defects resemble those caused by Ttk69 loss (Fig. 4G,J), although Ttk69 loss additionally causes some branching in the M3 layer (Fig. 4J). We conclude that Wnd acts cell-autonomously to disrupt R7 growth cone morphology during both halting and remodeling and that Wnd gain and Ttk69 loss cause similar remodeling

defects. We therefore speculated that Ttk69 might be responsible for the Hiw-independent repression of Wnd during this process.

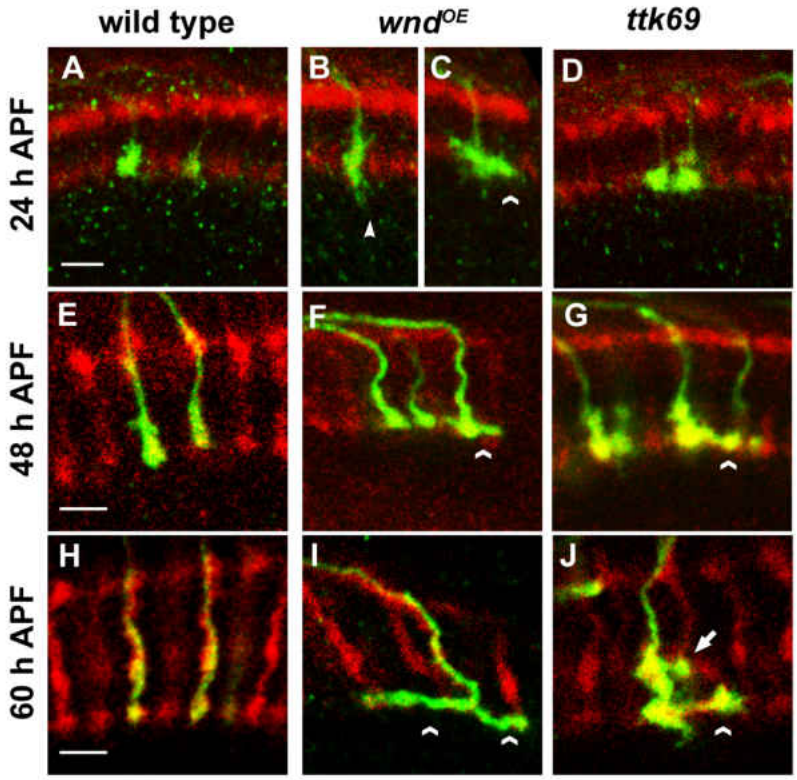

Figure 4. Wnd overexpression and Ttk69 loss cause similar defects in R7 growth cone remodeling.
(A-I) Pupal medullas (25°C) in which homozygous R7 clones generated by *GMR-FLP*/MARCM express mCD8-GFP (green). All R7 and R8 axons are labeled with anti-Chp (red). Scale bars are 5 µm. (A,E,H) Wild-type (homozygous *FRT82*) R7 axon terminals are roughly spherical at all time points and, by 60 h APF, rarely contact their neighbors (0.4±0.25%; n=11 brains). By contrast, at 24 h APF (B), R7s overexpressing Wnd have oblong axon terminals that partly extend beyond the R7 target layer (arrowhead), although some expand into neighboring terminals (C; chevron). During growth cone remodeling (F,I), R7s overexpressing Wnd have axon terminals that extend laterally and overlap with their wild-type neighbors (chevrons; 11.3±0.97% at 60 h APF; n=14). While *ttk69* mutant R7 growth cones are indistinguishable from wild type at 24 h APF (D), they also extend laterally and overlap with their wild-type neighbors in both the M6 (chevrons) and M3 (arrow) layers when they should instead be remodeling (G, J; 23.8±1.9% at 60 h APF; n=7).

Ttk69 acts in parallel with Hiw and JNK to decrease Wnd protein levels in R7 axon terminals during remodeling

To test whether Ttk69 might be responsible for the Hiw-independent repression of Wnd during growth cone remodeling, we measured anti-Wnd staining in wild-type and *ttkRNAi*-expressing R7 axon terminals at 48 and 60 h APF (Fig. 5A). We found that disrupting Ttk69 alone does not significantly increase Wnd expression at either timepoint (Fig. 5*A*). However, simultaneous loss of *hiw* and *ttk69* in R7s causes a striking increase in Wnd, well beyond the sum of that caused by loss of either alone (Fig. 5A), indicating that Hiw and Ttk69 act in parallel to repress Wnd. We conclude that Hiw and Ttk69 act redundantly in R7s to keep Wnd repressed during remodeling (Fig. 5C).

We next wondered whether JNK might also participate in repressing Wnd during remodeling, as it does during halting. We found that disrupting JNK in R7s does not measurably increase Wnd levels at 48 h APF (Fig. 5A). However, simultaneous disruption of JNK and Ttk69, like simultaneous disruption of Hiw and Ttk69, causes a synergistic increase in Wnd levels (Fig. 5A). We conclude that JNK continues to act in a negative feedback loop to restrict Wnd levels in R7 axon terminals during remodeling but, like Hiw, is redundant with Ttk69 during this process (Fig. 5C).

Finally, we wanted to test whether Ttk69, a transcriptional repressor, might directly regulate *wnd* transcription. To do so, we quantified and compared the levels of *wnd* mRNA in wild-type retinas and in retinas in which *chp-Gal4* drove expression of *UAS-ttkRNAi* in R neurons. We found no difference, despite being able to detect a significant difference between wild-type retinas and retinas in which *chp-Gal4* drove *UAS-wnd* (Fig. 5B). We conclude that Ttk69 is unlikely to repress Wnd directly, although it remains possible that there is a difference in *wnd* mRNA levels specifically in R7 neurons that we were unable to detect. We note that *wnd* mRNA levels do not detectably decrease in wild-type retinas during R7 remodeling (Fig. S3A in the Appendix), consistent with Ttk69 regulating Wnd only indirectly. We examined whether Ttk69 might regulate levels of *fat facets* mRNA, which encodes a deubiquitinase that acts in parallel with Hiw to regulate Wnd protein levels, but again we found no difference (Fig. S3B). We conclude that Ttk69 acts in parallel with Hiw but upstream of an unknown factor to repress Wnd in remodeling R7 growth cones (Fig. 5C).

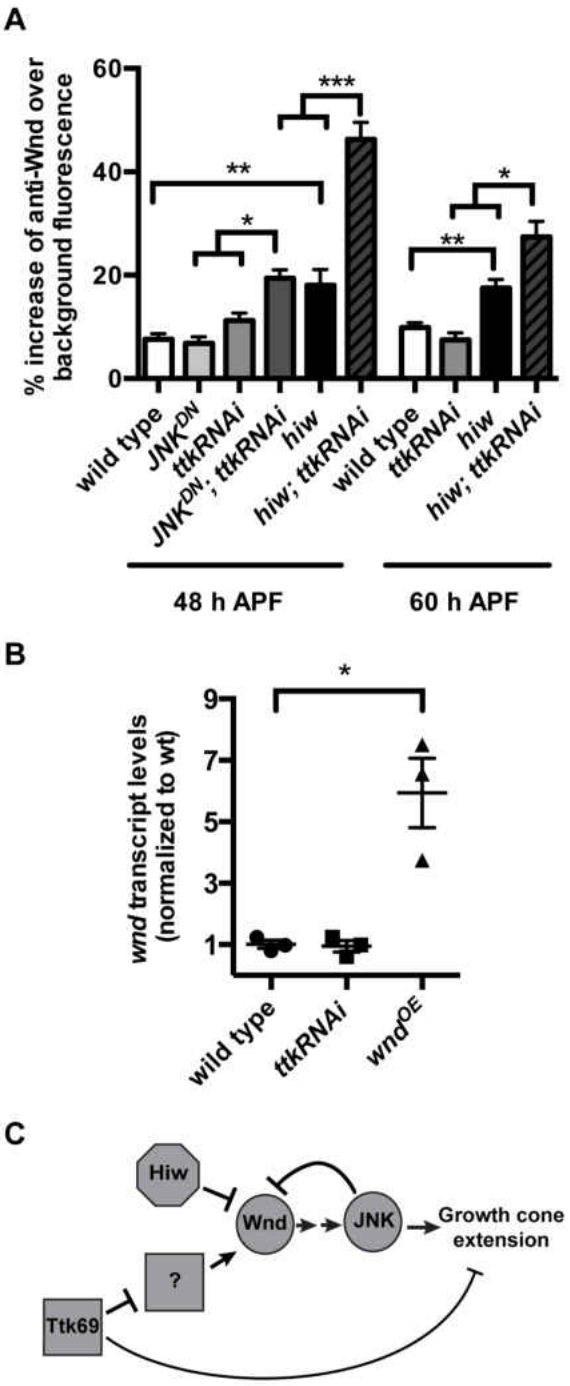

Figure 5. Specifically during R7 growth cone remodeling, Ttk69 acts in parallel with Hiw and JNK-dependent negative feedback to repress Wnd. (A) Quantification of anti-Wnd levels in R7 axon terminals at 48 and 60 h APF (29°C). n=brains, error bars represent SEM. n=19, 11, 12, 19, 15, 11, 16, 17, 8, and 11, respectively. Loss of *hiw* alone moderately increases Wnd levels in R7 axon terminals at both timepoints (note: values for wild type and *hiw* mutant at 60 h APF are reproduced from Fig. 1). Loss of *ttk69* alone (caused by *ttkRNAi*) has no significant effect on Wnd levels. However, loss of both *hiw* and *ttk69* causes a striking, significantly greater-than-additive increase in Wnd levels in R7 axon terminals at both timepoints. Similarly, loss of *JNK* alone (caused by JNK^{DN}) has no significant effect on Wnd levels, but loss of both *JNK* and *ttk69* causes a significantly greater-than-additive increase in Wnd levels in R7 axon terminals. *p<0.01, **p<0.001, and ***p<0.0001 based either on two-tailed t-tests for pairwise comparisons or a two-way ANOVA to test for greater than additive effects of disrupting two genes (Slinker, 1998). (B) Quantification of retinal *wnd* transcript levels measured by qRT-PCR. n=biological replicates, error bars represent SEM. Retinas in which all R neurons express *ttkRNAi* under the control of *chp-Gal4* have *wnd* transcript levels that are not significantly different from those in wild type; retinas in which R neurons express wnd under the control of *chp-Gal4* do have significantly increased *wnd* transcript levels. (C) Model summarizing the roles of Hiw, Wnd, JNK and Ttk69 in R7s as their growth cones remodel into presynaptic boutons.

During R7 growth cone remodeling, Wnd overexpression disrupts the reorientation of microtubule-containing processes and the downregulation of their extension and retraction rates

The DLK/JNK pathway is known to regulate microtubule organization and stability (Hirai et al., 2002; Hirai et al., 2006; Lewcock et al., 2007; Eto et al., 2010; Hendricks and Jesuthasan 2009; Hirai et al., 2011; Feltrin et al., 2012; Ghosh-Roy et al., 2012), but its specific effect on the transition from motile growth cone to stable presynaptic boutons has not been examined. Having established that increased Wnd disrupts this transition, we wanted to determine the mechanism in more detail. To do so, we caused R7s to express GFP-tagged EB1, which binds microtubule plus-ends (Rolls et al., 2007), and we imaged their axon terminals in live, *ex vivo* brains. We found that even in static images these live preparations allowed us to detect more details of R7 axon terminal morphology than are visible in fixed samples. We focused on two timepoints during the remodeling process. At 40 h APF, wild-type R7 axon terminals are still expanded (Fig. 6A,G), most have two or more EB1-GFP-containing processes of at least 0.5 μm extended at any given time (Fig. 6H), and these processes are primarily oriented at 180° relative to the axon shaft (Fig. 6I). By 48 h APF, wild-type R7 axon terminals have begun the remodeling process: they have condensed significantly (Fig. 6D,G), most have only one EB1-containing process (Fig. 6H), and that process is even more likely to extend directly forward (Fig. 6I). In addition, both the average extension and retraction rates of the EB1-containing processes decrease significantly between these two timepoints (Fig. 7A,B,G,H; Movies 1 and 2; all six movies can be found in a supplementary file as a companion to this dissertation).

We next quantified the behavior of R7s that overexpress Wnd. At 40 h APF their axon terminals are of normal size (Fig. 6B,G), and their EB1-containing processes have normal average extension and retraction rates (Fig. 7C,G,H, Movie 3). However, each terminal extends significantly more processes (Fig. 6H), and these processes are less apt to be oriented at 180° (Fig. 6I). By 48 h APF, Wnd-overexpressing R7 axon terminals have successfully condensed (Fig. 6E,G) and reduced their number of processes (Fig. 6H), similar to wild type. However, these processes remain less forward-oriented than in wild type (Fig. 6I) and fail to reduce their extension and retraction rates (Fig. 7D,G,H,

Movie 4). These results support a model in which Wnd does not specifically promote either microtubule assembly or disassembly in remodeling R7s but instead increases overall microtubule dynamism and disrupts microtubule orientation (Fig. 8).

Wnd overexpression and Ttk69 loss have overlapping but distinct effects on R7 growth cone remodeling

The R7 remodeling defects caused by Ttk69 loss are grossly similar to those caused by Wnd gain but are more frequent and more severe (Kniss et al., 2013). We wanted to distinguish whether this is because Ttk69 loss causes similar but more frequent and severe defects in microtubule dynamics or whether Ttk69 loss instead has distinct effects on microtubules. We found the latter to be true. Like Wnd overexpression, Ttk69 loss disrupts the forward reorientation of EB1-GFP-containing processes as R7 growth

---

Figure 6 (next page). Wnd overexpression and Ttk69 loss have overlapping but distinct effects on the morphology of remodeling R7 growth cones.
(A-F) Live R7 axon terminals labeled with *chp-Gal4, UAS-EB1-GFP* at 40 and 48 h APF (29°C) extend thin, EB1-GFP-positive processes (arrowheads). Driving *wnd* or *ttkRNAi* expression in R7s causes these processes to contact neighboring terminals (chevrons). Scale bars are 3 μm. (G-H) Quantifications of EB1-GFP-positive processes. n=terminals, error bars represent SEM. n= 20, 27, 30, 23, 22, 16, and 18, respectively. The areas of both wild-type (A,D) and *wnd*-overexpressing R7 axon terminals (B.E) decreases significantly during remodeling (compare 40 and 48 h APF; G). By contrast, loss of *ttk69* causes R7 axon terminals to increase in area (C,F,G). *baboRNAi*-expressing R7 axon terminals are abnormally large at 48 h APF but not as large as those expressing *ttkRNAi* (G). *$p<0.01$, **$p<0.001$, and ***$p<0.0001$ based on two-tailed t-tests. (H) *wnd* overexpression increases the number of EB1-GFP-positive R7 processes present at 40 h APF ($p<0.0001$ based on Fisher's Exact Test), but the number of these processes decreases to wild-type levels by 48 h APF. By contrast, *ttk69RNAi* causes an increase in process number that increases further by 48 h APF ($p<0.0001$ compared to wild type, Fishers Exact Test). R7s expressing *baboRNAi* have a wild-type number of processes at 48 h APF. Only processes ≥0.5 μm in length were counted. (I) Histogram plots of R7 process angles relative to the axon shaft. n=processes. Most wild-type EB1-GFP-positive processes point "forward" (at angles between 150° and 180°) even at 40 h APF (n=30), and the proportion that do so increases by 48 h APF (n=36). By contrast, R7s overexpressing *wnd* have a broader distribution of process angles at both timepoints, and the proportion that point forward does not increase between 40 (n=60) and 48 h APF (n=33). *ttk69RNAi* does not disrupt the primarily forward orientation of R7 processes at 40 h APF (n=45), but does so by 48 h APF (n=42). Finally, *baboRNAi* does not disrupt R7 process orientation even at 48 h APF (n=22). p values are based on Kolmogorov-Smirnov tests.

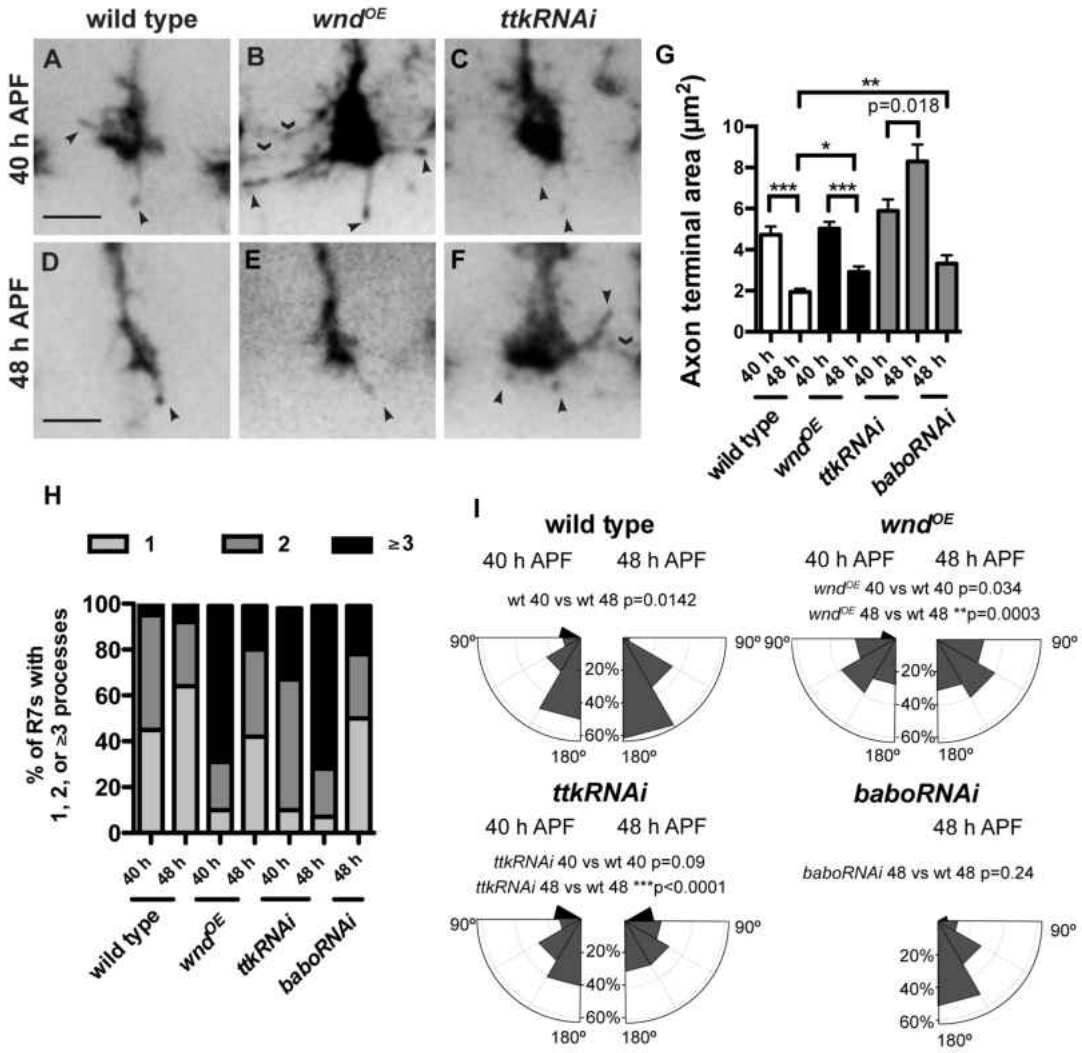
wild type
wnd^OE
ttkRNAi
A
B
C
D
E
F
40 h APF
48 h APF
G
Axon terminal area (µm²)
p=0.018
***
*
**
40 h
48 h
wild type
wnd^OE
ttkRNAi
baboRNAi
H
1
2
≥3
% of R7s with 1, 2, or ≥3 processes
I
wild type
40 h APF
48 h APF
wt 40 vs wt 48 p=0.0142
wnd^OE
wnd^OE 40 vs wt 40 p=0.034
wnd^OE 48 vs wt 48 **p=0.0003
ttkRNAi
ttkRNAi 40 vs wt 40 p=0.09
ttkRNAi 48 vs wt 48 ***p<0.0001
baboRNAi
baboRNAi 48 vs wt 48 p=0.24
90°
180°
20%
40%
60%

cones remodel (Fig. 6I) and prevents the normal reduction of process extension rate (Fig. 7F,G, Movie 5). However, unlike Wnd overexpression, Ttk69 loss also prevents R7 axon terminals from condensing (Fig. 6F,G), decreasing their number of EB1 processes (Fig. 6H), and does not prevent them from reducing their process retraction rate (Fig. 7F,H, Movie 6). Perhaps as a consequence, the length of EB1-containing processes increases significantly when Ttk69 is disrupted (Fig. 7I). We conclude that both Wnd overexpression and Ttk69 loss disrupt microtubule orientation and prevent the normal decrease in process extension, but that Ttk69 loss also promotes the continued formation and/or stabilization of microtubule-containing processes. We previously found that Ttk69 promotes R7 remodeling, in part, by promoting Activin/Baboon (Babo) signaling (Kniss et al., 2013). We therefore also examined the degree to which Babo loss resembled Ttk69 loss. We found that, like R7s expressing *ttkRNAi*, R7s expressing *baboRNAi* have an average extension rate that is significantly greater than wild type but an average process retraction rate that is indistinguishable from wild type (Fig. 7G,H). Ttk69's effect on Activin/Babo signaling may therefore account, in part, for its effect on R7 growth cone dynamics. However, we also found that Babo loss, unlike Ttk69 loss, does not increase average R7 process length (Fig. 7*I*) or number (Fig. 6*H*), confirming that Ttk69 does not act exclusively through this pathway. We conclude that Ttk69 is likely to coordinate the regulation of multiple factors that influence microtubule structure and dynamics during growth cone remodeling.

Figure 7 (next page). Wnd overexpression and Ttk69 loss have overlapping but distinct effects on the dynamics of remodeling R7 growth cones. (A-F) Images of live R7 axon terminals labeled with *chp-Gal4, UAS-EB1-GFP* at 40 and 48 h APF (29°C) at one minute intervals. Scale bars are 3 μm, arrowheads mark onsets of extensions, arrows mark onsets of retractions. In all genotypes, some processes remain stationary (asterisks). Processes that contact neighboring terminals (chevrons) were excluded from our analysis. (G-I) Quantifications of EB1-GFP-positive processes. n=processes, error bars represent SEM. *p<0.01, **p<0.001, ***p<0.0001 based on pairwise two-tailed t-tests. (G) n=37, 35, 26, 27, 44, 20, and 23, respectively. (H) n=34, 29, 24, 29, 42, 16, and 25, respectively. (I) n= 30, 36, 60, 33, 45, 42, and 22, respectively. The rates at which wild-type EB1-GFP-containing processes extend and retract decrease significantly during remodeling (compare 40 and 48 h APF; A,B,G,H). Wnd overexpression (C,D) prevents these decreases (G,H). Ttk69 loss (E,F) and Babo loss only prevent the decrease in extension rate (G,H). Ttk69 loss increases average process length (I).

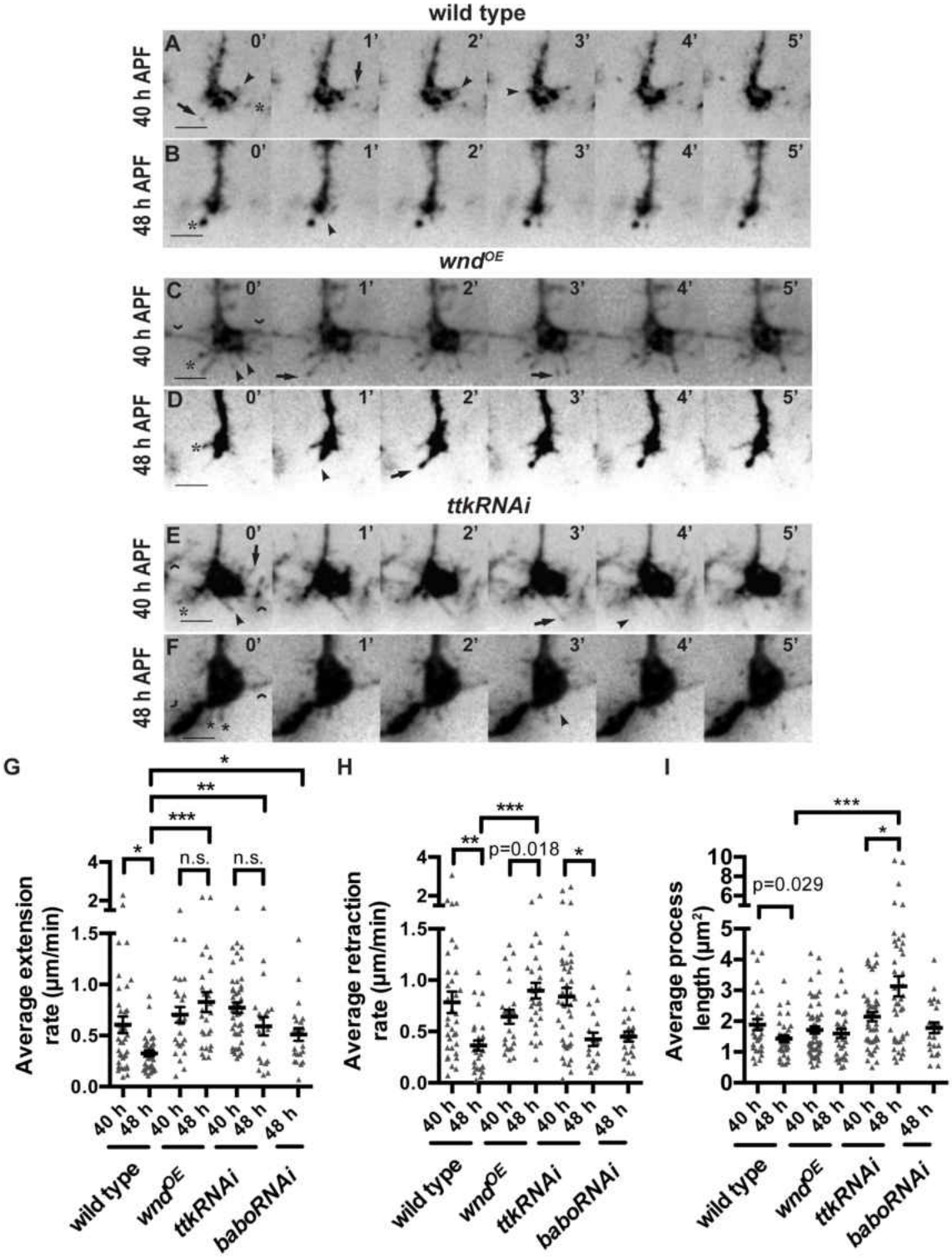
wild type
A
B
40 h APF
48 h APF
0'
1'
2'
3'
4'
5'
wndOE
C
D
ttkRNAi
E
F
G
H
I
Average extension rate (µm/min)
Average retraction rate (µm/min)
Average process length (µm²)
n.s.
p=0.018
p=0.029
40 h
48 h
wild type
wndOE
ttkRNAi
baboRNAi

Discussion

Wnd levels in developing R7s are temporally regulated by the transcription factor Ttk69

Elevated DLK protein levels enhance a neuron's ability to repair axon damage but impair its ability to form appropriate connections during development. DLK levels must therefore be carefully regulated. Here we show that, as has previously been observed in many systems, R7 neurons use a PHR protein, Hiw, to keep Wnd/DLK levels low enough for their growth cones to halt properly at their targets. However, we find that R7s later deploy a transcription factor, Ttk69, in parallel with Hiw to repress Wnd as their growth cones remodel into boutons. This progressive repression of DLK has not previously been reported but would make sense if growth cones become less tolerant of stochastic fluctuations in DLK as they become less motile. However, by adding PHR-independent mechanisms of DLK repression, maturing neurons would be predicted to express lower levels of DLK upon injury: in R7s, for example, Ttk69 would presumably continue to repress Wnd even if injury released Wnd from Hiw-mediated inhibition. In worm, the diminished capacity of older adults to recover from axon injury is caused by such a mechanism: as adult worms age, insulin/IGF-1 signaling represses DLK transcription, thereby limiting the increase in DLK after injury (Byrne et al., 2014). Our findings suggest that temporal control of DLK levels protects normal development even as it may limit regenerative capacity.

Wnd levels in R7s are repressed by JNK-mediated negative feedback

Like most signal transduction cascades, MAPK pathways can contain negative or positive feedback (Brummer et al., 2003; Fritsche-Guenther et al., 2011). In mouse neurons undergoing injury, JNK provides positive feedback within the DLK pathway by directly phosphorylating and thereby stabilizing DLK (Huntwork-Rodriguez et al., 2013). By contrast, here we show that in R7s JNK provides negative feedback within the DLK pathway by decreasing DLK protein levels. One possibility is that both positive and negative feedback co-exist in the DLK pathway in both mouse and fly. Negative feedback occurs during development, when the pathway must be restrained, whereas

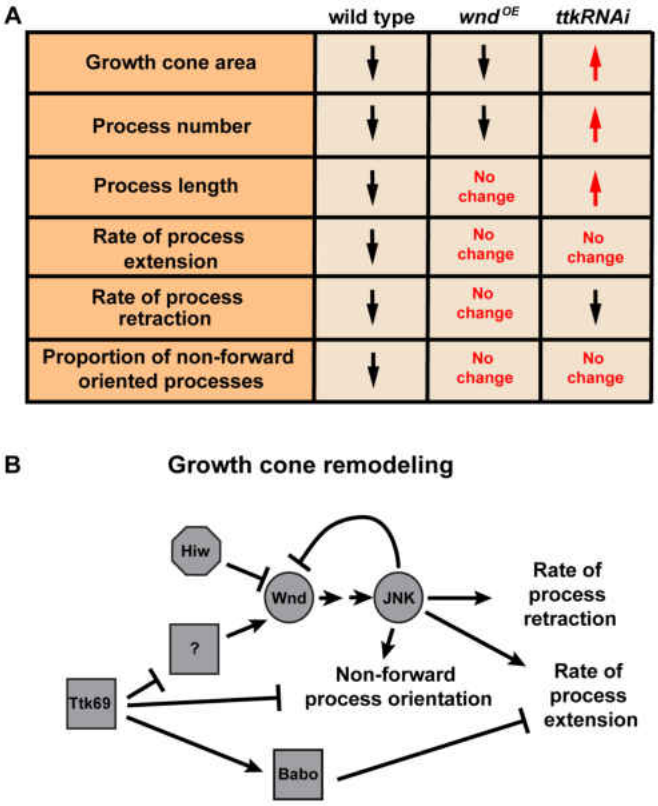

Figure 8. Model of how Wnd and Ttk69 affect the remodeling of R7 growth cones into presynaptic boutons.
(A) Table summarizing results from Fig. 6 and 7. In wild type, all properties listed decrease (black arrows). Wnd overexpression or Ttk69 loss causes some properties to increase (red arrows) or remain unchanged ("no change").
(B) Model consistent with the pathway relationships summarized in Fig. 5C and the phenotypes summarized in Fig. 8A, as well as with previous data on the pathway relationship between Ttk69 and Babo (Kniss et al., 2013) and the new data on Babo loss from Fig. 6 and 7.

positive feedback takes over upon injury, when there is a need to swiftly mount a sustained DLK response. Alternatively, our result may reflect a cell- or species-specific mechanism. In support of the latter possibility, the sites within mouse DLK that are phosphorylated by JNK are not conserved in fly Wnd (Huntwork-Rodrigues et al., 2013). However, we note that there is one conserved MAPK consensus phosphoryation site, S643 in mouse and S715 in fly, which remains a candidate for phosphorylation and consequent regulation by JNK in both species.

The R7 growth cone defect caused by Wnd overexpression changes over time

Wnd overexpression in R7s causes two distinct defects: their growth cones initially extend thin processes beyond their targets but later correct these and instead extend laterally. Each defect is similar to one observed in other systems [for example, Lewcock et al.,(2007) and Wang, et al., (2013), respectively]. However, why the defect changes over time is unclear. At each timepoint, the R7 growth cones maintain contact with their targets, consistent with previous work showing that DLK overexpression does not prevent growth cones from responding to extrinsic cues (Lewcock et al., 2007; Shin and DiAntonio, 2011). One possibility is that the extrinsic medullar environment initially allows Wnd-overexpressing R7 growth cones to send out forward-oriented processes but later constrains them, causing them to "burst out" laterally. Alternatively, the intrinsic R7 developmental program might be responsible - perhaps increased Wnd propels R7 axon shafts forward when R7 growth cones are already moving forward but has a different effect as the R7 terminals are attempting to remodel. This second possibility is consistent with evidence that the DLK can promote microtubule stability as well as instability and can switch from one to the other at different stages of a neuron's development (Hirai et al., 2011).

To examine this in more detail, we used live imaging of EB1-GFP to follow Wnd's effects on R7 microtubules. The high levels of EB1-GFP required to visualize R7s prevented us from observing "comets" (Morrison et al., 2002), but a comparison of our observations with a recent R7 study using a membrane-bound GFP (Özel et al*.,* 2015) suggests that even overexpressed EB1-GFP remains associated with microtubules: we counted far fewer GFP-positive processes than were observed with the membrane-bound GFP, and our processes extended and retracted at lower rates. We therefore believe our analysis reflects the behavior of pioneer microtubules, which escape the growth cone's central domain and explore a subset of growth cone filopodia (Lowery and Van Vactor, 2009; Bearce et al., 2015). We found that Wnd overexpression increases the number of EB1 processes in younger R7s (40 h APF), suggesting that Wnd initially promotes microtubule stability. However, Wnd does not prevent older R7 growth cones from condensing or decreasing their number of EB1 processes, suggesting that Wnd no longer promotes microtubule stability during remodeling. Indeed, Wnd appears to increase

overall microtubule dynamism at this later stage. Wnd's additional disruption of microtubule orientation could account for the lateral extensions, since the orientation of pioneer microtubules is strongly associated with the direction of growth cone consolidation (Bearce et al., 2015).

Ttk69 likely coordinates multiple pathways that regulate growth cone behavior

We performed several experiments to test the functional significance of the increased Wnd expression in R7s when both Hiw and Ttk69 are disrupted. We found that loss of *hiw* did not enhance the R7 defect caused by Ttk69 loss (Fig. S3C-I). Nor did disrupting Wnd or JNK ameliorate the R7 defect caused by Ttk69 loss (Fig. S3C-I). We also found that loss of *ttk69* and overexpression of Wnd have overlapping but distinct effects on the morphology and behavior of R7 growth cones. Together, these results are consistent with Ttk69 acting upstream of one or more additional regulators of growth cone dynamics that act in parallel with the Wnd/JNK pathway: in the absence of Ttk69, these other regulators severely disrupt R7 growth cone behavior whether or not Wnd is further increased or decreased (Fig. 8B).

CHAPTER III

WND LIKELY ACTIVATES CHANGES IN GENE EXPRESSION BY FOS AND IS REQUIRED FOR NORMAL SYNAPTIC BOUTON MORPHOLOGY

The work described in this chapter contains unpublished co-authored results. Alexander I. Feoktistov and Tory G. Herman designed and interpreted the experiments, while Kevin Kroeger and Alexander I. Feoktistov performed the experiments. Alexander I. Feoktistov wrote up the results.

Introduction

My work in Chapter II supports a model in which changes in neuronal expression of cell-intrinsic factors when neurons are establishing initial connectivity drive the transition from a motile growth cone to a stationary synaptic bouton. How might these factors accomplish this? Growth cone behavior is driven by rearrangements of the cytoskeleton, and there is evidence that both Ttk69 and DLK regulate signaling pathways that directly affect the actin and microtubule cytoskeletons, respectively. In this chapter I describe this evidence and present preliminary results from and future strategies for experiments attempting to identify the mechanisms by which expression of Wnd alters the organization or behavior of microtubules. I also discuss preliminary results that suggest that Wnd is not completely eliminated in wild type growth cones and plays a role in synapse assembly by the end of growth cone remodeling.

Does Wnd signaling cause biochemical changes in targets localized to the growth cone or are changes in gene expression required?

Like in other neurons studied (Hirai et al., 2002), Wnd is localized to the growth cone in R7s (See Figure 1 in Chapter II). DLK levels are also known to rise at the site of

injury after axotomy (Xiong et al., 2010); both results suggest that DLK acts locally within the growth cone. Supporting this, my work and past studies show that increased Wnd/DLK signaling causes dynamic changes in the behavior of the growth cone cytoskeleton, with my work showing that Wnd/DLK signaling promotes overall dynamism of microtubule-containing processes. Past work investigating the effect of excess DLK on microtubule behavior have shown sometimes conflicting results for the role of DLK in promoting microtubule stability but also instability. Evidence for DLK promoting microtubule stability comes from studies in regenerating worm neurons where excess DLK increases the frequency and duration of microtubule growth (Ghosh-Roy et al., 2012) and cultured zebrafish neurons with excessive DLK have increases microtubule velocities (Hendricks and Jesuthasan, 2009). Additionally defects in neurons crossing the midline in the zebrafish CNS expressing excessive DLK can be rescued by promoting microtubule catastrophe using the drug nocadozole (Hendricks and Jesuthasan, 2009). These results suggest that DLK promotes microtubule stability. Contradicting a simplistic model in which DLK simply promotes microtubule stability, work from mouse shows that inhibiting microutuble catastrophe with the drug taxol can rescue excessive DLK (Lewcock et al., 2007), consistent with DLK promoting microtubule instability. Further complicating this is work showing a context-dependent role for DLK in stabilizing microtubules during neurite formation, followed by axon extension (Hirai et al., 2011). Though my results do not fully resolve this controversy, it is clear that DLK signaling robustly affects the behavior of the growth cone cytoskeleton.

Local Wnd/DLK signaling can control microtubules through JNK-mediated phosphorylation of several microtubule regulators including microtubule associated proteins (MAPS) (Hirai et al., 2006; Eto et al., 2010; Feltrin et al.,, 2012; Coffey et al., 2014). This increases association of MAPs with microtubules (Hirai et al., 2006; Eto et al., 2010), promotes microtubule bundling (Feltrin et al., 2012, Klinedinst et al., 2013), and protects them from being severed. Kevin Kroger, a summer undergraduate student working with me in the Herman Lab, tested whether Wnd overexpression increased the abundance or disrupted the organization of the fly MAP1b Futsch, but he was unable to detect any difference between and MARCM-generated wild type and Wnd-overexpressing clones when staining for Futsch (data not shown). I also tested whether

DLK overexpression caused changes in immunostaining for acetylated microtubules, a marker of microtubule stability (Fukushima et al., 2009); however I saw no difference in abundance of this marker between MARCM-generated clones overexpressing Wnd (data not shown) and their wild type neighbors. In both of these cases, staining was widely distributed in the optic lobe, so it is possible that further optimization of the staining for ubiquitously expressed microtubules and associated proteins could detect subtle differences of these markers. Recent work in worm suggests that the microtubule severing protein Spastin acts downstream of DLK to generate dynamic microtubules during synapse remodeling (Kurup et al., 2015). I expressed RNAi against a fly microtubule severing protein called Spastin in R7s using *chp-Gal4*, but did not find any defects in R7 growth cone remodeling or axon morphology (data not shown). Additional genetic experiments manipulating expression of other candidate genes like a related microtubule severing protein katanin or cytoplasmic linker proteins (CLIPS) might reveal potential targets of Wnd signaling acting locally within growth cones (Dent et al., 2011).

DLK signaling activates MAPKs that can phosphorylate target proteins in the axon, but MAPKs also phosphoactivate transcription factors triggering changes in gene expression. DLK signaling in developing or regenerating neurons activates the transcription factors Fos and/or CEBP downstream of JNK and/or p38, respectively (Lindwall et al, 2004; Yan et al*.,* 2009, Itoh et al., 2009; Shin et al., 2012; Hirai et al., 2011). Indeed, Fos is required for DLK signaling to exert its effects in both developing and regenerating neurons (Collins et al., 2006; Xiong et al., 2010; Watkins et al., 2013, Wang et al., 2013). To test whether Fos is required for defects in growth cone remodeling caused by excessive DLK, I expressed a dominant negative version of Fos (fos^{DN}) in R7s also overexpressing Wnd using *chp-Gal4*. This largely rescued the excessive axon overextension caused by Wnd overexpression with only occasional R7s extending axons into neighboring terminals (chevron in Fig. 9C), showing that Wnd requires functional Fos and thus likely exerts much of its effects by causing changes in gene expression. Curiously, there was also an enhancement of a phenotype I had only occasionally observed in R7s overexpressing Wnd or lacking Hiw. R7s that are both overexpressing Wnd and express fos^{DN} often retract from their appropriate target layer (arrow in Fig. 9C). R7s expressing fos^{DN} (Fig. 9A) do not appear to have this confounding phenotype. I

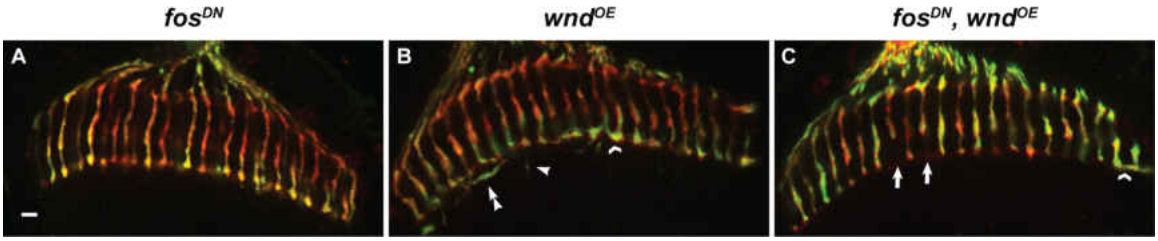

Figure 9. Wnd overexpression requires the transcription factor Fos.
(A-C) Young adult medullas (29°C) in which R7 and R8 axons are labeled with *chp-Gal4* expressing *UAS-eb1-GFP* (green), and anti-Chp (red). scale bar= 5 µm. Fos^{DN} expressing R7s (A) largely resemble wild type (not shown). R7s overexpressing *wnd* in adult medullas (B) by contrast frequently extend into neighboring terminals within their target layers (chevrons). Unlike younger R7s expressing *wnd* (see Chapter II), R7s overexpressing *wnd* in adults frequently extend axons in layers other than the R7 target layer (double arrowheads in B). These R7s also extend long projections beyond their target layer (arrowheads). R7s expressing both fos^{DN} and overexpressing *wnd* (C) only occasionally extend into neighboring terminals (chevron), but expressing both transgenes causes frequent retraction of R7s from their target layer (arrows in C).

had sometimes observed R7s retracted from their target layer in R7s with excess Wnd in 60 h APF pupae and adults, but I had also occasionaly scored wild type R7s as having this phenotype in my genotype-blind quantification. The small differences were not significant (data not shown), thus I was unable to clearly identify a cause for this rare phenotype.

One clue suggesting why R7s lacking Hiw or overexpressing Wnd retract from their target layers is that this phenotype occurs more often in more mature R7s. Perhaps the inability of R7s overexpressing Wnd to remodel into synaptic boutons as described in Chapter II means they progressively lose attachment with their target layer. This could be supported in part by another apparent difference in phenotypes of younger R7s described in my study above and the older ones described in this chapter –R7s overexpressing Wnd in adult animals frequently extend processes and branches within and through proximal target layers (double arrowheads in Fig. 9B), which were not seen in younger R7s. However this does not explain why loss of *fos* would enhance this particular defect. Perhaps any potential effect of Wnd overexpression on contact with the target layer is due to local effects at the growth cone or axon terminal, and subsequent gene expression by Fos triggers a feedback mechanism that normally maintains attachment to the target

layer. However, there is little evidence directly supporting such speculation without a clear idea about what changes in gene expression are driven by Fos.

To determine what genes are activated by Fos downstream of Wnd, relative transcript abundance of candidate genes involved in signaling pathways that act on the cytoskeleton can be tested by performing qRT-PCR on transcripts from retinas where Fos is either inactivated by expression of a dominant negative or activated by expression of Wnd using *chp-gal4* and comparing these genetic manipulations to wild type and to each other. Though there is lingering concern about the sensitivity of this technique in detecting minor changes in transcript abundance due to the fact that only a subset of the many cells in the retina are being genetically manipulated by *chp-Gal4,* in the course of my study described in Chapter II, I was able to detect a significant increase Wnd transcripts in retinas expressing Wnd driven by *chp-Gal4*. Because Fos does seem to be required for the effect of excess Wnd on growth cone remodeling, it is likely that Wnd overexpression would cause similarly significant changes in gene expression that could be detected. A role for Fos can be established by comparing transcripts of retinas overexpressing Wnd alone to retinas overexpressing Wnd and expressing fos^{DN}. Thus concerns about transcripts from non-genetically manipulated support cells of the retina diluting potential differences between transcripts from genetically manipulated photoreceptors should not discourage pursuing this strategy. Cost is another issue, so more efficient methods like RNAseq may be better suited to finding any overlooked genes that are strongly regulated by Fos downstream of Wnd. Further studies on Wnd-Fos target genes identified using this strategy could be used to confirm or reject a causative role in the phenotypes seen in R7s overexpressing Wnd.

Wnd is required by the end of growth cone remodeling for normal synaptic bouton morphology

Thus far, my work shows that Hiw and a JNK-mediated negative feedback set limits on Wnd expression levels during R7 growth cone halting and that expression of Ttk69 at the time R7s begin remodeling their growth cones into synaptic boutons sets an additional limit on Wnd during this subsequent developmental time window. However, a

requirement for Wnd in R7 development was not apparent in my study described in Chapter II, consistent with other studies showing only subtle defects, if any, in neurons lacking DLK (Collins et al., 2006; Fernandes et al., 2011; Shin and DiAntonio, 2011; Wang et al., 2013.) For example, only upon subsequent re-analysis of bouton morphology and staining for specific markers was the requirement of Wnd in fly NMJs identified (Collins et al., 2006; Klinedinst et al., 2013). Thus I was intrigued when acquiring images of *wnd* null brains at 60 h APF for normalization of anti-Wnd staining intensity, and I noticed that R7s in these brains frequently extended thin processes of uniform width (arrowheads Fig. 10B) that resemble phenotypes the Herman lab and others, have detected in R7s lacking genes known to promote assembly of the site of synaptic vesicle release in presynaptic cells (Astigarraga et al., 2010; Holbrook et al., 2012), which is called the active zone (AZ). Because the entire brain lacked *wnd* it is possible that this defect is non cell-autonomous.

An interpretation for why R7s with defects in AZ assembly extend ectopic processes is that a lack of functional signaling at the presynapse causes R7s to create ectopic sprouts and perhaps contacts with improper targets. It is possible that any number of defects in development of synaptic targets of R7s in the optic lobe could cause R7s to exhibit this phenotype. Thus, to determine cell-autonomy, it is necessary to generate MARCM clones of R7s lacking *wnd*. These tools are readily available, and experiments

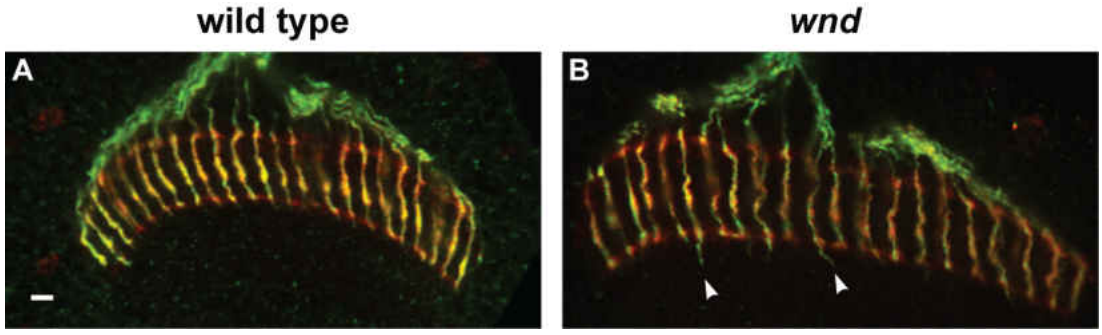

Figure 10. Wnd is required by the end of growth cone remodeling for normal synaptic bouton morphology.
(A,B) 60 h APF pupal medullas (29°C) in which R7s and R8s are labeled by expressing *chp-Gal4, UAS-mCD8-GFP* (green) and anti-Chp (red). scale bar= 5 µm. Wild type R7s (A) have ellipsoid boutons that do not extend beyond their target layers. R7s in *wnd* null brains often extend thin, uniformly wide ectopic sprouts beyond their target layer (arrowheads in B).

to clarify this question are ongoing at the time of this writing. Thus it seems likely that Wnd is required for development of neurons in the developing pupal brain, much like at the fly NMJs. If Wnd is found to be required cell-autonomously in R7s, further work would be required to determine if Wnd acts through JNK-Fos or, if like at the fly NMJ, Wnd acts through p38 to disrupt Futsch organization (Klinedinst et al., 2013). This could be tested by genetic experiments to test whether animals missing one copy of *wnd* and one copy of *p38, JNK,* or *fos* produce ectopic sprouts more frequently than heterozygous mutant animals alone. Pursuing such a study would provide greater insight into changing regulation and function of the neuronal cytoskeleton of the neuronal cytoskeleton during development.

CHAPTER IV

HOW DOES TEMPORAL EXPRESSION OF TTK69 PROMOTE GROWTH CONE REMODELING?

The work described in this chapter contains unpublished co-authored results. Alexander I. Feoktistov and Tory G. Herman designed and interpreted the experiments, while Alex Whitebirch and Alexander I. Feoktistov performed the experiments. Alexander I. Feoktistov wrote up the results.

Is there a functional consequence to an absence of repression of Wnd by both Ttk69 and Hiw?

My study described in Chapter II shows that Ttk69 cooperates with Hiw to repress Wnd protein levels, however, the functional consequence of this regulation is not clear from the above study. While I was able to detect an increase in Wnd protein levels in the absence of both Ttk69 and repression by Hiw or JNK-mediated negative feedback, I was unable to detect an effect of increasing or decreasing Wnd signaling on the frequency with which R7s extend into neighboring columns. The latter is readily explained by the fact that Ttk69 is known to regulate additional pathways that contribute to this phenotype (see below). However, I was surprised that the increase in Wnd levels caused by loss of both *hiw* and *ttk69* did not further increase the frequency of R7s extending into neighboring columns, particularly since overexpressing Wnd is sufficient to cause this. One possibility is that my ability to detect an increase in this phenotype is confounded by the method. Expressing *ttkRNAi* in all R7s obscures the source of an extending axon, thus when multiple laterally-extending axons overlap, they are undercounted. Compared to my quantification of MARCM-generated clones lacking Ttk69, I repeatedly counted half as many R7s extending into neighboring columns that were all expressing *ttkRNAi*..

Another possibility is that the frequency with which R7s lacking Ttk69 extend into neighboring terminals reaches a maximum. Ttk69 is first detected in photoreceptor cell bodies at 30 h APF, and by 36h APF, R7s lacking Ttk69 first begin extending into neighboring columns. By 48 h APF the frequency of R7s lacking Ttk69 extending axons into neighbors doubles and plateaus (Kniss et al., 2013). I asked whether there might be a genetic interaction between Ttk69 and Hiw at 36 h APF, when the phenotype was not yet maximal. R7 growth cones in *hiw* null brains mostly resemble wild type growth cones which are ellipsoid and have mostly separated into discrete, non-overlapping columns. However, some R7s in *hiw* null brains extend processes beyond their target layer (Fig. 11A) and a handful are elongated (Fig. 11B), much like the phenotype seen at 24 h APF, but these defects are not significantly more frequent in *hiw* null brains than wild type. Additionally I was able to detect some R7s in *hiw* mutant brains extending into neighboring columns (Fig 11A), though again, this was not significantly more frequent than in wild type. Expressing *ttkRNAi* using *chp-Gal4* also caused R7s to exhibit all three of these phenotypes, though again the frequency was not significantly greater than in wild type (Fig 11A-C.). However, R7s expressing *ttkRNAi* in *hiw* null brains causes a significant increase of all three of the above phenotypes when compared to wild type. Additionally, R7s expressing *ttkRNAi* in *hiw* null brains extend processes beyond their target layer more frequently and are less circular than R7s in *hiw* null brains or those expressing *ttkRNA* alone. Though R7s expressing *ttkRNAi* in *hiw* null brains are significantly more likely to extend into neighboring columns than R7s expressing *ttkRNAi* alone, they are not more likely to do so than R7s in *hiw* null brains (Fig. 11A-C). The apparent genetic interaction between Ttk69 and Hiw is consistent with my model presented in Chapter II in which repression of Wnd by both Hiw and Ttk69 helps reduce growth cone motility during remodeling. Thus, I would expect that a synergistic increase of Wnd protein levels in the absence of repression by both Hiw and Ttk69 would explain the genetic interaction between these two genes. However, when I measured anti-Wnd intensity in these growth cones, I saw no difference in levels of Wnd in R7s expressing *ttkRNAi* in *hiw* null brains compared to R7s in *hiw* null brains (Fig 11D). Thus the genetic interaction between Hiw and Ttk69 in terms of R7 growth cone behavior cannot be explained by a synergistic increase in Wnd protein levels. These findings are based on an

initial round of dissections which yielded a small sample of *hiw* null brains, thus it is possible that I lack the power to detect changes in Wnd protein levels until this experiment can be repeated.

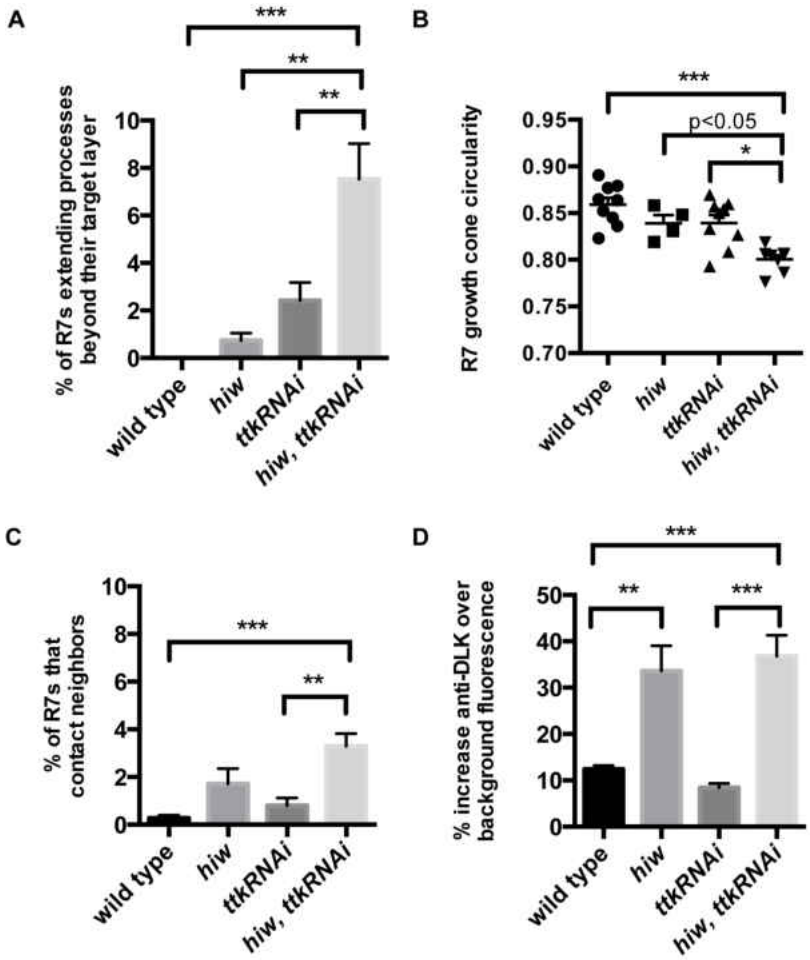

Figure 11. Loss of both *hiw* and *ttk69* enhances loss of function phenotypes caused by loss of either alone without a synergistic effect on Wnd protein levels. (A-D) Quantification of the frequency of wild type,R7s extending processes beyond their target layer (A), average growth cone circularity (B), the frequency of R7s that contact neighbors (C) and anti-Wnd intensity of wild type, *hiw* null, *ttkRNAi*-expressing, and both *hiw* null and *ttkRNAi*-expressing R7s in 36 h APF pupal medullas (29°C). n=brains, error bars represent SEM n=9, 4, 9, and 8, respectively. R7s that lack either *hiw* or *ttk69* alone are not more significantly likely to extend processes beyond their target layer (A), have non-circular growth cone morphology (B) or extend processes into neighboring terminals than wild type(C). By contrast, R7s that lack both *ttk69* and *hiw* are more likely to extend processes beyond their target layer (A), are less circular (B) and more frequently contact neighbors than wild type R7s. Despite this, there is not a significant increase in anti-Wnd levels in R7 terminals of R7s lacking both *ttk69* and *hiw* than R7s lacking *hiw* alone. *p<0.01, **p<0.001, ***p<0.0001 based on Sidak's multiple comparison test

A persistent concern about our ability to reproducibly measure anti-Wnd protein intensity is being able to detect changes in Wnd protein levels in *hiw* null brains compared to other genotypes. While most of our other manipulations using *chp-Gal4* affect R7 terminals without affecting the adjacent neuropil, *hiw* null brains have increased Wnd everywhere, including the adjacent neuropil. Because this adjacent neuropil was used as way to normalize for variability in staining, this distorts my measurements of Wnd protein intensity in *hiw* null brains. Though it is unlikely that this would severely disrupt our interpretations in Chapter II (for explanation, see Figure S1 legend in the Appendix), it is possible that this would obscure subtle differences in Wnd protein levels. One way to simultaneously address this concern and likely undercounting of R7s contacting neighbors when all R7s lack Ttk69 is to generate R7 clones using MARCM that are both *hiw* null and expressing *ttkRNAi.* This experiment is technically difficult because of the need to combine multiple transgenes in one animal, but the individual tools required to accomplish this task are presently available. By comparing R7 clones lacking *hiw*, expressing *ttkRNAi*, or both to their wild type neighbors, a reliable internal control can be used to detect more subtle difference in Wnd protein levels between these genotypes and thus establish a causative relationship between phenotype and Wnd protein levels. Furthermore, the use of clones would allow more reliable quantification of the frequency of R7s extending laterally, as well as other aspects of the phenotype caused by loss of *ttk69*, specifically the length of axons that extend laterally within the R7 target layer. In R7s lacking Ttk69, this latter phenotype does not plateau, but continues to increase while R7s are normally remodeling into stable synaptic boutons. These experiments could reveal the functional consequence of a lack of repression of Wnd by both Ttk69 and Hiw during growth remodeling.

How does Ttk69 regulate the behavior of the growth cone cytoskeleton?

It is known that Ttk69 promotes signaling downstream of the fly Type I TGF-β receptor Baboon (Babo), and is required for entry of phosphorylated Smad into the nucleus of R7s (Kniss et al., 2013). Babo signaling is required to prevent R7s from extending into neighboring terminals (Ting et al., 2007), though it is known that Ttk69

also promotes growth cone remodeling through effects on other pathways. I found that expressing *baboRNAi* in using *chp-Gal4* increases the rate of extension of microtubule-containing processes in R7 growth cones compared to wild type. Expressing *ttkRNAi* in R7s also causes increased rates of extension of microtubule-containng processes compared to wild type, suggesting that Ttk69 restricts process extension during growth cone remodeling by promoting Babo signaling.

How might Babo signaling then affect the growth cone cytoskeleton? Work on fly mushroom body neurons suggests that Babo has Smad-independent roles in preventing axon overextension. Instead Babo requires RhoGTPase signaling to LIMK to do so (Ng, 2008). LIMK phosphorylates and inactivates the actin-severing molecule cofilin. Cofilin is thought to promote axon growth by promoting actin tread milling; linking actin filaments to the membrane by integrin and associated scaffolds and signaling proteins provides the propulsive force for the growth cone (Lowery and Van Vactor, 2009). In an attempt to test specific effects of expressing *ttkRNAi* or *baboRNAi* on the dynamic behavior of the actin cytoskeleton, I expressed the actin-binding protein moesin tagged with GFP in living R7s. While axons were visible, overall intensity of GFP expression appeared reduced and it was difficult to detect discrete filopodia at R7 terminals (data not shown). Thus direct visualization of dynamic behavior of actin-based structure was not possible. Because of the considerable cross-talk between the actin and microtubule cytoskeleton, however, it is likely that decreasing actin tread milling could create space for unhindered entry of microtubules into the growth cone filopodia (Stiess and Bradke, 2011) and promoting axon extension (Stiess and Bradke, 2011; Bearce et al., 2015).

How then does Ttk69 promote Babo signaling? Studies attempting to answer this question were carried out by Alex Whitebirch under my supervision. Due to the Smad-independent role of Babo in preventing axon overextension in fly mushroom bodies, we looked at candidate genes which could affect Babo signaling. Follistatin is a conserved molecule that blocks the ability of Babo to bind its ligand Activin. Alex expressed RNAi against Follistatin in R7 clones lacking Ttk69 generated by MARCM, but was unable to detect a decrease in the frequency of R7s extending into neighboring columns as would be expected were Ttk69 normally required to repress Follistatin. It is possible that varied genetic interaction experiments with R7s lacking Ttk69 are repeatedly fruitless due to the

strong effect Ttk69 clearly has on growth cone development. Thus it seems like a strategy focusing on changes in gene expression caused by loss of *ttk69* would be a more productive.

Now that I have verified that qRT-PCR can detect large changes in gene expression driven by *chp-Gal4* in photoreceptor neurons despite the diluting effect of transcripts from retinal cells other than photoreceptor, a possible strategy would be to detect changes in candidate gene transcript abundance between wild type retinas and retinas expressing *ttkRNAi* using *chp-Gal4*. Validating the likely utility of this technique, I have generated preliminary evidence suggesting that Ttk69 might repress transcription of the repulsive netrin receptor unc-5, which we are investigating as the cause for the related R8 photoreceptors failing to extend to their final targets when expressing *ttkRNAi* using *chp-Gal4* (data not shown). Thus I was able to detect changes in gene expression of a single cell type among the eight photoreceptor types despite dilution by both their and other retinal cells' transcript pools. Applying qRT-PCR or more cost efficient transcript profiling techniques to identify Ttk69 targets could reveal other conserved signaling pathways and proteins like TGF-β or DLK that cell-intrinsically regulate the dynamic rearrangements of growth cones.

CHAPTER V

CONCLUSIONS

Altogether my work builds support for a model in which a decrease in growth cone motility when neurons establish connectivity is driven by changes in expression of cell-intrinsic factors. I showed that protein levels of the conserved MAP3K Wnd/DLK are limited first by Hiw/PHR and a JNK-mediated feedback loop during growth cone halting, followed by additional repression of Wnd by Ttk69 after its expression is activated. There have been some reports of a decrease in DLK expression in neurons progressing through development (Eto et al., 2010), with some effects attributed to a temporal role of Hiw during growth cone halting (Collins et al., 2006). It is intriguing to speculate whether other neurons use additional mechanisms to set limits on the amount of DLK that is expressed or active when it is released from inhibition by PHR, which is what happens upon axon severing (Hammarlund et al., 2009; Xiong et al., 2010). It is known that a decrease in DLK transcription due to inhibition of FOXO by insulin reduces the regenerative capacity of aging worm neurons (Byrne et al., 2014). Of clinical relevance is the question of whether cell-intrinsic differences in the amount of DLK that is expressed in the absence of inhibition by Hiw can account for cell-intrinsic differences in the ability of neurons to regenerate. An affirmative answer to this question could provide targets for therapies, as DLK is both necessary and sufficient for regeneration in multiple model systems.

While Ttk69 is not a conserved protein, the effect of transcription factors in regulating the ability to regenerate a motile growth cones in mammalian nervous systems is established (Moore and Goldberg, 2011). Might Ttk69 share common targets with vertebrate transcription factors? Being able to trigger changes in expression of multiple genes simultaneously, transcription factors are potentially powerful drivers of coordinated remodeling to the machinery that characterizes motile growth cones. Understanding how the profound changes in a neuron's morphology over its development are coordinated so that a stereotyped circuitry is assembled will allow us to re-activate this program to promote therapies design to repair circuits damaged by injury or disease.

CHAPTER VI

MATERIALS AND METHODS

Fly husbandry. *Drosophila melanogaster* were raised at either 25°C (Fig. 2 A-F, Fig. 3*A-F'*, and Fig. 4) or 29°C (Fig.1, Fig. 2G, Fig 3G, H and Figs. 5-7). We used both sexes and observed no difference The following strains were used in this study: "wild type" were *Oregon R, yw*, or *w*; "*hiw* mutant" were $hiw^{\Delta N}$ or hiw^{AC} hemizygous males, or $hiw^{\Delta N}$/ hiw^{AC} or $hiw^{\Delta N}/hiw^{ND8}$ transheterozygous females (Wu et al., 2005); "*wnd* mutant" were wnd^{1}/wnd^{3} transheterozyogous animals (Collins et al., 2006). Flies expressing the following transgenes were also used: *chaoptin* (*chp*)-*Gal4* (a generous gift from S. L. Zipursky, University of California, Los Angeles, CA), *actin* (*act*)-*Gal4* (Bloomington *Drosophila* Stock Center), *PM181-Gal4* (Lee et al., 2001), *UAS-wnd* (wnd^{OE}; Collins et al., 2006), *UAS-*Bsk^{DN} (JNK^{DN}; Weber et al., 2000), *UAS-mCD8-ChRFP* (Bloomington *Drosophila* Stock Center), *UAS-Dcr-2* (Dietz *et al* 2007), *UAS-mCD8-GFP* (Lee and Luo, 1999), and *UAS-EB1-GFP* (Rolls et al., 2007). *UAS-RNAi* lines from the Vienna *Drosophila* Resource Center were used to knock down expression of Ttk69 (#101980) and Babo (#106092). Homozygous wild type (*FRT82*), *ttk69* mutant (ttk^{1e11}; Xiong and Montell, 1993), or *UAS-wnd* overexpressing R7 clones were generated and labeled using *GMR-FLP* and MARCM (mosaic analysis with a repressible cell marker; Lee and Luo, 1999; Lee et al., 2001).

Fixed images. Brains were dissected, fixed, and stained by standard methods (Miller et al., 2008). Staining was done in parallel with controls, and phenotypes were scored blind. Images were collected on a Leica SP2 microscope and analyzed using Fiji (http://fiji.sc; Schindelin *et al*., 2012). We used the following antibodies: mouse anti-Chp (24B10; 1:200) from the Developmental Studies Hybridoma Bank; rabbit anti-Wnd (A3-1,2; 1:300; Collins et al., 2006), a generous gift from C. Collins; chicken anti-GFP (1:1000) from Abcam, rabbit anti-GFP (1:5000) and all secondary antibodies (goat IgG coupled to Alexa Fluor 488, Alexa Fluor 555, or AlexFluor 633; 1:250) from Life Technologies.

To quantify Wnd protein, we generated regions of interest (ROIs) by tracing ~20 R7 terminals per optic lobe while blind to the anti-Wnd channel (Fig. S1A-B'). We then measured anti-Wnd fluorescence intensities within these ROIs. To control for variability in immunostaining, we normalized the average anti-Wnd intensity in R7s of each brain to the average anti-Wnd fluorescence intensity of adjacent medulla neuropil (Fig. S1A-C). All images, ROIs, and raw data are available upon request.

Live images. We adapted the protocol of Williamson and Hiesinger (2010). Briefly, animals were minimally dissected in HL3 (Broadie 2000): each pupa was removed from its case and its head isolated with visual system intact. For 40 h APF brains, no further dissection was required. For 48 h APF brains, further removal of cuticle from the posterior head was often necessary for optical access. The brains were then transferred in HL3 along with fat bodies to imaging chambers (Cabernard et al., 2013) and immobilized using WormGlu (Glushield) on gas-permeable membranes (YSI). Brains were mounted dorsal-side down and images acquired from the ventral, posterior part of the medulla at a depth of three or four R7 axon terminals. We used a Leica DMI400B spinning disk microscope to image ~3 μm z-stacks (acquired in 0.3 μm z-steps) at 30-second intervals during a 30-minute period. Images were processed using Fiji: we generated max projections of 7-10 z-steps encompassing the total thickness of an R7 terminal and corrected for lateral drift using TurboReg. The length of each process was measured from the edge of the pixel-dense growth cone to the tip of each projection. Discrete extension and retraction events (defined as a change in length of at least 0.5 μm) were identified manually, and the lengths of processes at the beginning and the end of each event (defined as a pause or a reversal in direction) were measured to determine average rates (calculated by dividing the change in length by the change in time during a given event). Instantaneous velocity was not measured. All images and raw data are available upon request.

Quantitative RT-PCR. qRT-PCR was performed using KAPA SYBR FAST ABI Prism qPCR master mix (Kapa Biosystems) on cDNA synthesized using oligo $(dT)_{18}$ primer and Maxima H-Minus reverse transcriptase (Thermo Scientific). cDNAs were generated

from 1 μg of Trizol-isolated RNA from 10-20 pairs of dissected pupal retinas per biological replicate. Retinas were dissected on ice, and tissue was flash frozen in Trizol. Relative mRNA expression was normalized using a control transcript (Rpl32) to calculate ΔCTs (threshold cycles). Expression level comparisons between genetic manipulations or developmental timepoints were made using the ΔΔCT method. ΔCT values were used for two-tailed t-tests to determine statistical significance. The following primer sequences (5' → 3') were used for qPCR in this study.

Rpl32 Forward: CTAAGCTGTCGCACAAATGGC

Rpl32 Reverse: TTGCGCTTCTTGGAGGAGAC

Wnd Forward: GGCAGGCTAAAGAACGAGACT

Wnd Reverse: CCAAGCGGGACGGTAACAT

Faf Forward: GTGGACAGCACCATCACAATAG

Faf Reverse: CACAAGGATACAGTGGTGGATGT

APPENDIX A

SUPPLEMENTARY FIGURES AND LEGENDS

Figure S1 (next page). Details on how anti-Wnd staining in R7 growth cones was quantified.
(A-B') *hiw* mutant pupal medullas (25°C) in which R7 and R8 are labeled with (A,B) *chp-Gal4, UAS-EB1-GFP* (green) and anti-Chp (red) and (A',B') anti-Wnd. Abnormal R7 processes (arrowheads) are more strongly labeled with anti-Chp than by *chp-Gal4, UAS-EB1-GFP*. At both 24 (A') and 60 h APF (B'), anti-Wnd staining was quantified by using anti-Chp alone to trace both R7 growth cones (magenta dotted lines in A-B') as well as an adjacent but distinct region of neuropil (white dotted lines in A-B'). The level of anti-Wnd staining within each R7 tracing was then measured and compared to the average level of anti-Wnd staining within the adjacent region. (C) Quantification of average fluorescence intensities within the R7-adjacent neuropil (white dotted lines in A-B'). n= brains, error bars represent SEM. n= 14, 19, 16, 10, 12, and 17, respectively. There is no significant change in anti-Wnd staining in this region in wild type; our use of this region to normalize the anti-Wnd staining within R7 growth cones therefore does not confer or obscure temporal differences in wild-type R7s. There is a significant decrease in anti-Wnd staining in this region in *hiw* mutant animals between 24 and 60 h APF, suggesting that a temporal, Hiw-independent mechanism might also repress Wnd in medulla axons. Our use of this region to normalize the anti-Wnd staining within *hiw* mutant R7 growth cones does not invalidate our finding that a Hiw-independent, Ttk69-dependent mechanism represses Wnd in *hiw* mutant R7 growth; however, it may cause an underestimate of the strength of this Hiw-

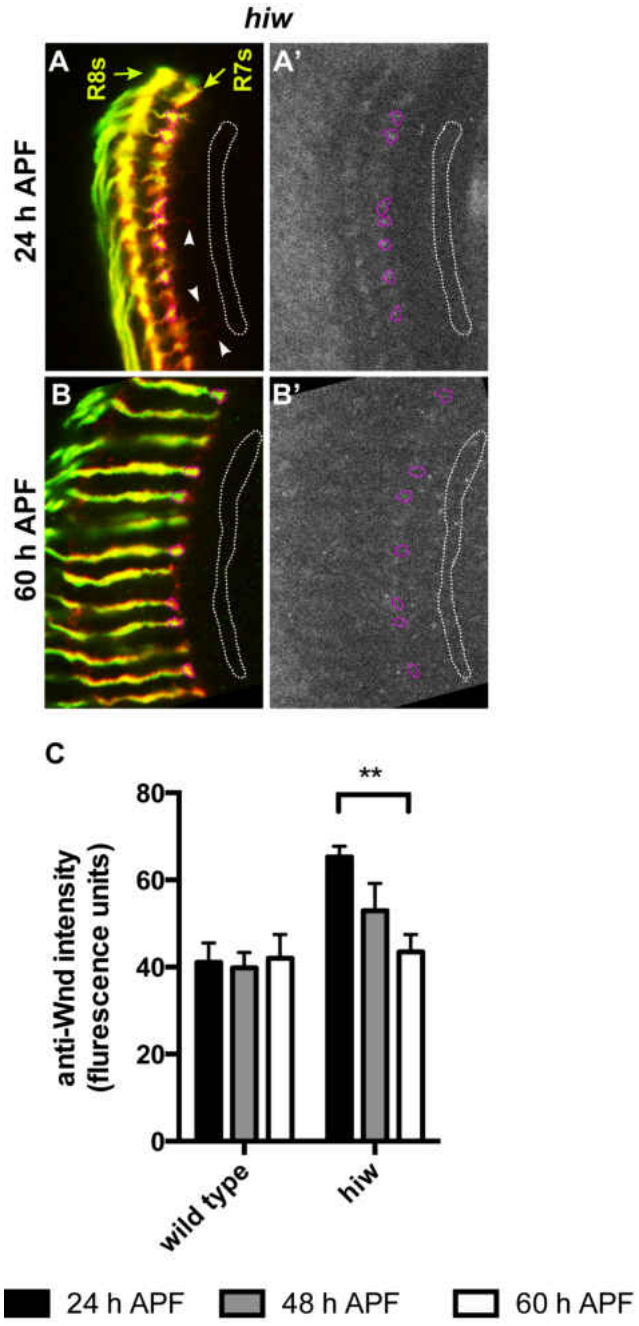
hiw
A
R8s
R7s
A'
24 h APF
B
B'
60 h APF
C
**
80
60
40
20
0
anti-Wnd intensity
(flurescence units)
wild type
hiw
24 h APF
48 h APF
60 h APF

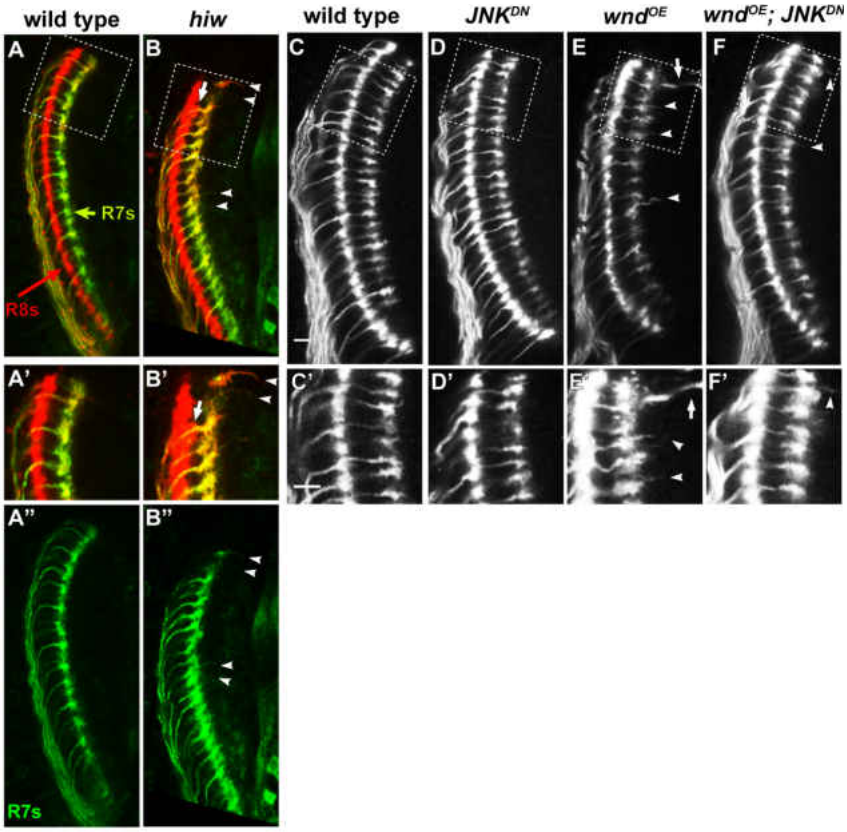

Figure S2. Wnd disrupts layer-specific R7 growth cone halting through JNK.
(A-B") 24 h APF pupal medullas (25°C) in which R7 axons are specifically labeled with *PM181-Gal4, UAS-mCD8-GFP* (green), and both R7 and R8 axons are labeled with anti-Chp (red). A' and B' are enlargements of the boxed regions in A and B with brightness enhanced so that thin growth cone processes are visible. The R7-specific labeling confirms that it is the R7s in *hiw* mutants that extend processes beyond their target layer (arrowheads) and that it is not R7s that occasionally terminate between the R8 and R7 target layers (arrow in B and B' pointing to growth cone between R8 and R7 target layers that is stained red but not green).
(C-F'), 24 h APF pupal medullas (29ºC), in which R7 and R8 axons are labeled with *chp-Gal4, UAS-EB1-GFP* (white) . Scale bars are 5 µm. (C'-F') are enlargements of the boxed regions in (C-F) with enhanced brightness. R7 growth cones expressing dominant-negative JNK (JNK^{DN}; D,D') are indistinguishable from wild type (C,C'). R7 growth cones expressing wild-type Wnd (Wnd^{OE}; E,E') extend processes beyond their target layer (arrowheads); these processes resemble those in *hiw* mutants but sometimes extend deeper into the optic lobe (arrows). Co-expressing JNK^{DN} with wild-type Wnd almost completely ameliorates this defect (F,F', arrowheads indicate some remaining abnormal processes). These phenotypes are quantified in Fig. 2G.

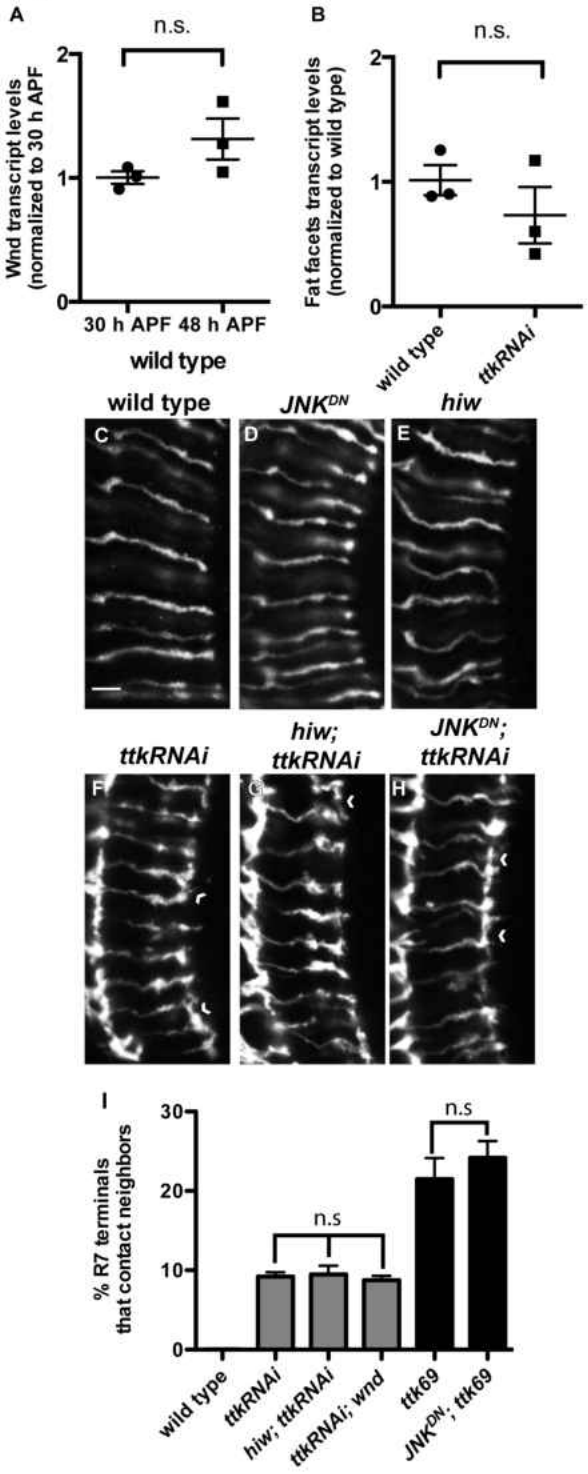

Figure S3. Ttk69 regulates Wnd protein expression indirectly and regulates additional pathways to promote R7 growth cone remodeling. (A,B) Quantifications of transcript levels measured by qRT-PCR on RNA extracted from dissected retinas. n= 3 biological replicates, and error bars represent SEM. (A) There is no detectable change in *wnd* mRNA levels as R7 growth cone remodeling progresses. (B) Loss of *ttk69* from R neurons does not detectably increase *fat facets* (*faf*) mRNA levels. (C-H) 48 h APF pupal medullas (29°C) in which R7 and R8 axons are labeled with *chp-Gal4, UAS-EB1-GFP*. Scale bars are 5 μm. (I) Quantification of the frequency with which R7 axon terminals contact their neighbors. n=brains and error bars represent SEM. n.s. not significant based on a pairwise two-tailed t-test. n=17, 22, 11, 10, 5, and 9, respectively. Wild-type (C), JNK^{DN}-expressing (D), and *hiw* mutant R7 axon terminals (E) are indistinguishable. The frequency with which R7s expressing *ttkRNAi* contact their neighbors (F; chevrons) is not increased by additional loss of *hiw* (G,I). And loss of *JNK* (caused by expressing JNK^{DN}; H) or *wnd* (I) from *ttkRNAi*-expressing R7s does not ameliorate this defect. Similarly, disrupting *JNK* in *GMR-FLP*-generated *ttk69* mutant R7s (by causing them to express JNK^{DN}) does not ameliorate this defect. Note that contacts between individually-labeled *GMR-FLP*-generated *ttk69* mutant R7 axon terminals and their neighbors are easier to score than contacts among uniformly labeled R7 axon terminals, so the frequency of this defect is scored as much higher in the former situation.

APPENDIX B

MULTIMEDIA LEGENDS

Spinning disk confocal movies, each spanning 30 minutes of real time, sped up 300x (10 frames were collected every 30 seconds but are here presented at 1 frame/second). See Methods for imaging conditions.

Movie 1. Representative wild-type R7 axon terminal at 40 h APF.

Movie 2. Representative wild-type R7 axon terminal at 48 h APF. The average extension and retraction velocities of processes are reduced compared to 40 h APF.

Movie 3. Representative wnd^{OE} R7 axon terminal at 40 h APF. The average extension and retraction velocities of processes are indistinguishable from those in wild type at 40 h APF.

Movie 4. Representative wnd^{OE} R7 axon terminal at 48 h APF. The average extension and retraction velocities of processes are greater than those in wild type at 48 h APF.

Movie 5. Representative *ttkRNAi*-expressing R7 axon terminal at 40 h APF. The average extension and retraction velocities of processes are indistinguishable from those in wild type at 40 h APF.

Movie 6. Representative *ttkRNAi*-expressing R7 axon terminal at 48 h APF. The average retraction velocity of processes is indistinguishable from that in wild type at 48 h APF; however, the average extension velocity of processes is greater than that in wild type at 48 h APF.

REFERENCES CITED

Astigarraga, S., Hofmeyer, K., Farjian, R., and Treisman, J.E. (2010) Three Drosophila liprins interact to control synapse formation. J. Neurosci 17;30(46): 15358-68

Baker, S. T., Opperman, K. J., Tulgren, E. D., Turgeon, S. M., Bienvenut, W., & Grill, B. (2014). RPM-1 uses both ubiquitin ligase and phosphatase-based mechanisms to regulate DLK-1 during neuronal development. PLOS Genet., 10(5), e1004297.

Bearce, E. A., Erdogan, B.,& Lowery, L. A. (2015) TIPsy tour guides: how microtubule plus-end tracking proteins facilitate axon guidance. Fron Cell Nerusoci., 9:241.5

Bloom, A. J., Miller, B. R., Sanes, J. R., & DiAntonio, A. (2007). The requirement for Phr1 in CNS axon tract formation reveals the corticostriatal boundary as a choice point for cortical axons. Genes Dev, 21(20), 2593–2606.

Brace, E. J., Wu, C., Valakh, V., & DiAntonio, A. (2014). SkpA restrains synaptic terminal growth during development and promotes axonal degeneration following injury. J. Neurosci., 34(25), 8398–8410.

Brummer, T., Naegele, H., Reth, M., & Misawa, Y. (2003). Identification of novel ERK-mediated feedback phosphorylation sites at the C-terminus of B-Raf. Oncogene, 22(55), 8823–8834.

Broadie, K. (2000) Electrophysiological approaches to the neuromusculature. In: *Drosophila* Protocols (Sullivan, W., Ashburner, M., & Hawley, R. S., ed) pp 274-275. Cold Spring Harbor, NY: CSHLP.

Burgess, R. W., Peterson, K. A., Johnson, M. J., Roix, J. J., Welsh, I. C., & O'Brien, T. P. (2004). Evidence for a conserved function in synapse formation reveals Phr1 as a candidate gene for respiratory failure in newborn mice. Mol. Cell. Biol., 24(3), 1096–1105.

Byrne, A. B., Walradt, T., Gardner, K. E., Hubbert, A., Reinke, V., & Hammarlund, M. (2014). Insulin/IGF1 signaling inhibits age-dependent axon regeneration. Neuron, 81(3), 561–573.

Case, L. C., and Tessier-Lavigne, M. (2005) Regeneration of the adult central nervous system. Curr. Biol. 15(18), 20 September. R749-R753.

Cabernard, C., & Doe, C. Q. (2013). Live imaging of neuroblast lineages within intact larval brains in Drosophila. Cold Spring Harb. Protoc., 2013(10), 970–977.

Chen, C.-H., Lee, A., Liao, C.-P., Liu, Y.-W., & Pan, C.-L. (2014). RHGF-1/PDZ-RhoGEF and retrograde DLK-1 signaling drive neuronal remodeling on microtubule disassembly. Proc. Natl. Acad. Sci. U.S.A., 111(46), 16568–16573.

Chen, Y., Akin, O., Nern, A., Tsui, C. Y. K., Pecot, M. Y., & Zipursky, S. L. (2014). Cell-type specific labeling of synapses in vivo through synaptic tagging with recombination. Neuron, 81(2), 280–293.

Coffey, E. T. (2014) Nuclear and cytosolic JNK signaling in neurons. Nature Rev (155, 285-299.

Collins, C. A., Wairkar, Y. P., Johnson, S. L., & DiAntonio, A. (2006). Highwire restrains synaptic growth by attenuating a MAP kinase signal. Neuron, 51(1), 57–69.

D'Souza, J., Hendricks, M., Le Guyader, S., Subburaju, S., Grunewald, B., Scholich, K., & 694 Jesuthasan, S. (2005). Formation of the retinotectal projection requires Esrom, an ortholog of PAM (protein associated with Myc). Development, 132(2), 247–256.

Dietzl, G., Chen, D., Schnorrer, F., Su, K.-C., Barinova, Y., Fellner, M., Gasser, B., Kinsey, K., Oppel, S., Scheiblauer, S., Cuoto, A., Marra, V., Keleman, K., & Dickson, B. J. (2007). A genome-wide transgenic RNAi library for conditional gene inactivation in Drosophila. Nature, 448(7150), 151–156.

Eto, K., Kawauchi, T., Osawa, M., Tabata, H., & Nakajima, K. (2010). Role of dual leucine zipper-bearing kinase (DLK/MUK/ZPK) in axonal growth. Neurosci. Res., 66(1), 37–45.

Feltrin, D., Fusco, L., Witte, H., Moretti, F., Martin, K., Letzelter, M., Fluri, E., Scheiffele, P., & Pertz, O.(2012). Growth cone MKK7 mRNA targeting regulates MAP1b-dependent microtubule bundling to control neurite elongation. PLoS Biol., 10(12), e1001439.

Fernandes, K. A., Harder, J. M., John, S. W., Shrager, P., & Libby, R. T. (2014). DLK-710 dependent signaling is important for somal but not axonal degeneration of retinal ganglion cells following axonal injury. Neurobiol. Dis., 69, 108–116.

Fritsche-Guenther, R., Witzel, F., Sieber, A., Herr, R., Schmidt, N., Braun, S., Brummer, T., Sers, C., & Blüthgen, N. (2011). Strong negative feedback from Erk to Raf confers robustness to MAPK signalling. Mol. Syst. Biol., 7, 489.

Fukishima, N. Furua, D., Hidaka, Y., Moriyaama, R., Tsujiuichi, T. (2009) Post-translational modifications of tubulin in the nervous system. J. Neurchem 109(3): 683-93.

Ghosh-Roy, A., Goncharov, A., Jin, Y., & Chisholm, A. D. (2012). Kinesin-13 and tubulin posttranslational modifications regulate microtubule growth in axon regeneration. Dev. Cell, 23(4), 716–728.

Godement, P., Wang, L. C., & Mason, C. A. (1994). Retinal axon divergence in the optic chiasm: dynamics of growth cone behavior at the midline. J. Neurosci., 14(11 Pt 2), 7024–7039.

Goldberg, J. L. (2004). Intrinsic neuronal regulation of axon and dendrite growth. Curr. Opin. Neurobiol., 14(5),

Grill, B., Bienvenut, W. V., Brown, H. M., Ackley, B. D., Quadroni, M., & Jin, Y. (2007). C. elegans RPM-1 regulates axon termination and synaptogenesis through the Rab GEF GLO-4 and the Rab GTPase GLO-1. Neuron, 55(4), 587–601.

Hammarlund, M., Nix, P., Hauth, L., Jorgensen, E. M., & Bastiani, M. (2009). Axon regeneration requires a conserved MAP kinase pathway. Science (New York, N.Y.), 323(5915), 802–806.

Hendricks, M., & Jesuthasan, S. (2009). PHR regulates growth cone pausing at intermediate targets through microtubule disassembly. J. Neurosci., 29(20), 6593–6598.

Hendricks, M., Mathuru, A. S., Wang, H., Silander, O., Kee, M. Z. L., & Jesuthasan, S. (2008). Disruption of Esrom and Ryk identifies the roof plate boundary as an intermediate target for commissure formation. Mol. Cell Neurosci, 37(2), 271–283.

Hirai, S.-I., Kawaguchi, A., Hirasawa, R., Baba, M., Ohnishi, T., & Ohno, S. (2002). MAPK upstream protein kinase (MUK) regulates the radial migration of immature neurons in telencephalon of mouse embryo. Development, 129(19), 4483–4495.

Hirai, S.-I., De Feng Cui, Miyata, T., Ogawa, M., Kiyonari, H., Suda, Y., Aizawa, S., Banba, Y., & Ohno, S. (2006). The c-Jun N-terminal kinase activator dual leucine zipper kinase regulates axon growth and neuronal migration in the developing cerebral cortex. J. Neurosci., 26(46), 11992–12002.

Hirai, S.-I., Banba, Y., Satake, T., & Ohno, S. (2011). Axon formation in neocortical neurons depends on stage-specific regulation of microtubule stability by the dual leucine zipper kinase c-Jun N-terminal kinase pathway. J. Neurosci., 31(17), 6468–6480.

Hoffman, P. N. A conditioning lesion induces changes in gene expression and axonal transport that enhance regeneration by increasing the intrinsic growth state of axons. Exp Neurol. 223(1), 11-18

Holbrook, S., Finley, J.. K., Lyons, E. L., and Herman, T. G. (2012) Loss of syd-1 from R7 neurons disrupts two distinct phases of presynaptic development. J. Neursci Dec 12; 32(50):1801-11.

Huntwork-Rodriguez, S., Wang, B., Watkins, T. A., Ghosh, A. S., Pozniak, C. D., Bustos, D., Newton, K., Kirkpatrick, D. S., & Lewcock, J. W. (2013). JNK-mediated phosphorylation of DLK suppresses its ubiquitination to promote neuronal apoptosis. J. Cell Biol., 202(5), 747–763.

Klinedinst, S., Wang, X., Xiong, X., Haenfler, J. M., & Collins, C. A. (2013). Independent pathways downstream of the Wnd/DLK MAPKKK regulate synaptic structure, axonal transport, and injury signaling. J. Neurosci., 33(31), 12764–12778.

Kniss, J. S., Holbrook, S., & Herman, T. G. (2013). R7 photoreceptor axon growth is temporally controlled by the transcription factor Ttk69, which inhibits growth in part by promoting transforming growth factor-β/activin signaling. J. Neurosci., 33(4), 1509–1520.

Kurup, N., Yan., D., Goncharov, A., Jin, Y., (2015)Dynamic microtubules drive circuit rewiring in the absence of neurite remodeling. Curr Biol 25(12): 1594-1605.

Langen, M., Agi, E., Altschuler, D. J., Wu, F., Altschuler, S. J., Hiesinger, P. R., (2015) The developmental rules of neural superposition in *Drosophila*. Cell, 162(2): 120-33.

Lee, C. H., Herman, T. G., Clandinin, T. R., Lee, R., & Zipursky, S. L. (2001). N-cadherin regulates target specificity in the Drosophila visual system. Neuron, 30(2), 437–450.

Lee, T., & Luo, L. (1999). Mosaic analysis with a repressible cell marker for studies of gene function in neuronal morphogenesis. Neuron, 22(3), 451–461.

Lewcock, J. W., Genoud, N., Lettieri, K., & Pfaff, S. L. (2007). The ubiquitin ligase Phr1 regulates axon outgrowth through modulation of microtubule dynamics. Neuron, 56(4), 604– 779 620.

Li, H., Kulkarni, G., & Wadsworth, W. G. (2008). RPM-1, a Caenorhabditis elegans protein that functions in presynaptic differentiation, negatively regulates axon outgrowth by controlling SAX-3/robo and UNC-5/UNC5 activity. J. Neurosci., 28(14), 3595–3603.

Liao, E. H., Hung, W., Abrams, B., & Zhen, M. (2004). An SCF-like ubiquitin ligase complex 786 that controls presynaptic differentiation. Nature, 430(6997), 345–350.

Lowery, L. A., & Van Vactor, D. (2009). The trip of the tip: understanding the growth cone machinery. Nat. Rev. Mol. Cell Biol., 10(5), 332–343.

Mar, F. M., Bonni, A., & Sousa, M. M. (2014). Cell-intrinsic control of axon regeneration. EMBO rep., 15(3), 254–263.

McCabe, B. D., Hom, S., Aberle, H., Fetter, R. D., Marques, G., Haerry, T. E., Wan, H., O'Connor, M. B., Goodman, C. S., & Haghighi, A. P. (2004). Highwire regulates presynaptic BMP signaling essential for synaptic growth. Neuron, 41(6), 891–905.

Miller, A. C., Seymour, H., King, C., & Herman, T. G. (2008). Loss of seven-up from Drosophila R1/R6 photoreceptors reveals a stochastic fate choice that is normally biased by Notch. 800 Development, 135(4), 707–715.

Moore, D. L., & Goldberg, J. L. (2011). Multiple transcription factor families regulate axon 803 growth and regeneration. Dev. Neurobiol., 71(12), 1186–1211.

Morrison, E. E., Moncur, P. M., & Askham, J. M. (2002). EB1 identifies sites of microtubule polymerisation during neurite development. Brain Res. Mol. Brain Res., 98(1-2), 145–152.

Nakata, K., Abrams, B., Grill, B., Goncharov, A., Huang, X., Chisholm, A. D., & Jin, Y. (2005). Regulation of a DLK-1 and p38 MAP kinase pathway by the ubiquitin ligase RPM-1 is required for presynaptic development. Cell, 120(3), 407–420.

Nix, P., Hisamoto, N., Matsumoto, K., & Bastiani, M. (2011). Axon regeneration requires coordinate activation of p38 and JNK MAPK pathways. Proc. Natl. Acad. Sci. U.S.A, 108(26), 10738–10743.

Ng, J. (2008); TGFβ signals regulate axonal development through distinc Smad-indeprendent mehcanisms. Development 135: 4025-4035.

Opperman, K. J., & Grill, B. (2014). RPM-1 is localized to distinct subcellular compartments and regulates axon length in GABAergic motor neurons. Neural Dev., 9:10.

Özel, M. N., Langen, M., Hassan, B. A., Hiesinger, P. R. (2015). Filopodial dynamics and growth cone stabilization in *Drosophila* visual circuit development. eLife 2015;10.7554/elife.10721.

Schaefer, A. M., Gayla, H. D., & Nonet, M. L. (2000) *rpm-1*, A conserved neuronl gene that regulates targeting and synaptogenesis in *C. elegans*. Neuron, 26(2): 345-356.

Schindelin, J., Arganda-Carreras, I., & Frise E., Kaynig, V., Longair, M., Pietzsch, T., Preibisch S., Rueden, C., Saalfield, S., Schmid, B, et al. (2012) Fiji: an open-source platform for biological-image analysis. Nat Methods., 9(7): 672-82.

Rolls, M. M., Satoh, D., Clyne, P. J., Henner, A. L., Uemura, T., & Doe, C. Q. (2007). Polarity and intracellular compartmentalization of Drosophila neurons. Neural Dev., 2:7.

Sharma, J., Baker, S. T., Turgeon, S. M., Gurney, A. M., Opperman, K. J., & Grill, B. (2014). Identification of a Peptide Inhibitor of the RPM-1·FSN-1 Ubiquitin Ligase Complex. J. Biol. Chem., 289(50), 34654–34666.

Shin, J. E., & DiAntonio, A. (2011). Highwire regulates guidance of sister axons in the Drosophila mushroom body. J. Neurosci., 31(48), 17689–17700.

Shin, J. E., Cho, Y., Beirowski, B., Milbrandt, J., Cavalli, V., & DiAntonio, A. (2012). Dual leucine zipper kinase is required for retrograde injury signaling and axonal regeneration. Neuron, 74(6), 1015–1022.

Steketee, M. B., Oboudiyat, C., Daneman, R., Trakhtenberg, E., Lamoureux, P., Weinstein, J. E., Heidemann, S., Barres, B. A., & Goldberg, J. L. (2014). Regulation of intrinsic axon growth ability at retinal ganglion cell growth cones. Invest. Ophthalmol. Vis. Sci., 55(7), 4369–4377.

Stiess, M. and Bradke, F. (2011), Neuronal polarization: The cytoskeleton leads the way. Devel Neurobio, 71: 430–444. doi: 10.1002/dneu.20849

Tedeschi, A., & Bradke, F. (2013). The DLK signalling pathway-a double-edged sword in Neural Dev. and regeneration. EMBO rep., 14(7), –614.

Ting, C.-Y., Yonekura, S., Chung, P., Hsu, S.-N., Robertson, H. M., Chiba, A., & Lee, C.-H. (2005). Drosophila N-cadherin functions in the first stage of the two-stage layer-selection process of R7 photoreceptor afferents. Development, 132(5), 953–963.

Ting, C.-Y., Herman T., Ynekura, S., Gao, S., Wang, J., Serpe, M., O'Connor, M. B. Zipursky, S.L and Lee, C.-H. (2007) Tiling of r7 axons in the Drosophila visual system is mediated by both transcduction of an activing signal to the nucleus and mutual repulsion. Neuron Dec 6; 56(5): 793-806

Vitriol, E. A., & Zheng, J. Q. (2012). Growth cone travel in space and time: the cellular ensemble of cytoskeleton, adhesion, and membrane. Neuron, 73(6), 1068–1081.

Weber, U., Paricio, N., & Mlodzik, M. (2000). Jun mediates Frizzled-induced R3/R4 cell fate distinction and planar polarity determination in the Drosophila eye. Development, 127(16), 3619–3629.

Wang, X., Kim, J. H., Bazzi, M., Robinson, S., Collins, C. A., & Ye B. (2013) Bimodal control of dendritic and axonal growth by the dual leucine zipper kinase pathway. PLoS Biol. 11(6) p. e1001572

Watkins, T. A., Wang, B., Huntwork-Rodriguez, S., Yang, J., Jiang, Z., Eastham-Anderson, J., Modrusan, Z., Kaminker, J. S., Tessier-Lavigne, M., and Lewcock, J. (2013) DLK initiates a transcriptional program that couples apoptotic and regenerative responses to axonal injury. Proc Natl Acad Sci USA. Mar 5;110 (10): 4039-44.

Williamson, W. R. & Hiesinger, P. R. (2010) Prepation of developing and adult *Drosophila* brains and retinae for live imaging. J Vis Exp. (37): 1936.

Wu, C., Daniels, R. W., & DiAntonio, A. (2007). DFsn collaborates with Highwire to down regulate the Wallenda/DLK kinase and restrain synaptic terminal growth. Neural Dev., 2:16.

Wu, C., Wairkar, Y. P., Collins, C. A., & DiAntonio, A. (2005). Highwire function at the Drosophila neuromuscular junction: spatial, structural, and temporal requirements. J. Neurosci., 25(42), 9557–9566.

Xiong, W. C., & Montell, C. (1993). tramtrack is a transcriptional repressor required for cell fate determination in the Drosophila eye. Genes Dev, 7(6), 1085–1096.

Xiong, X., Wang, X., Ewanek, R., Bhat, P., DiAntonio, A., & Collins, C. A. (2010). Protein 880 turnover of the Wallenda/DLK kinase regulates a retrograde response to axonal injury. J. Cell Biol., 191(1), 211–223.

Yan D., Wu, Z., Chisholm, A. D., & Jin, Y. (2009) The DLK-1 kinase promotes mRNA stability 884 and local translation in *C. elegans*. Cell., 138(5), 1005-1018.

Yan, D., & Jin, Y. (2012). Regulation of DLK-1 kinase activity by calcium-mediated dissociation 887 from an inhibitory isoform. Neuron, 76(3), 534–548.